Accumulation of γKetoaldehyde-modified Protein in Normal and Fibrotic Lung

By

Stacey Mont

Dissertation
Submitted to the Faculty of the
Graduate School of Vanderbilt University
in partial fulfillment of the requirements
for the degree of

DOCTOR OF PHILOSOPHY
in

Cancer Biology
August, 2016
Nashville, Tennessee

Approved:

Michael Freeman, PhD

Timothy Blackwell, MD

William Lawson, MD

Linda Sealy, PhD

TABLE OF CONTENTS

LIST OF TABLES

LIST OF FIGURES

Figure Page

CHAPTER I

INTRODUCTION

Generation of γKetoaldehydes

Arachidonic acid is a 20-carbon lipid molecule and is a major component of biological membranes. Free arachidonic acid, not bound to phospholipids, has been historically studied within the context of cyclooxygenase (COX) activity[1]. COX can act directly with arachidonic acid forming Prostaglandin-H2 (PGH2). This endoperoxide intermediate can then form several lipid products including, TXA2, PGI1, PGD2, PGF2, and PGE2 (see figure 1)[2].

Phospholipid esterified arachidonic acid can react with free radicals and non-enzymatically undergo lipid peroxidation forming Prostaglandin-H2-like molecules termed Isoprostanes. Isoprostanes as the name implies are isomeric structures of prostaglandins due to containing the same prostane ring structure. Isoprostanes can rearrange in a similar fashion as Prostaglandin-H2, to form E2-, D2-, A2-, J2-isoprostanes, and isothromboxanes[3] (see figure 1).

Both the cyclooxygenase pathway and the free radical oxygenation of arrachidonic acid form γKetoaldehydes (γKAs). The γKAs arising from the isoprostane pathway are also known as isoketals (isoKs) to emphasize how they are isomers of γKAs[4]. The γKAs arising from the prostaglandin pathway are also known as levuglandins[5]. The term isolevuglandins (isoLGs) has been also used and as isoketals were termed to emphasize how they are isomeric molecules of levuglandins[6]. Free radical oxidation with arachidonic acid is fast occurring and enzyme independent and

thus it is believed that the majority of γKAs generated in-vivo are generated by the isoprostane pathway (see figure 1)[2].

γKetoaldehydes regardless of origin (COX derived or free radical derived) are highly reactive lipid molecules due to their unstable open-ring structure, which has a high avidity to lysine residues. This reaction forms covalent pyrrole adducts which further stabilizes into lactam adducts on proteins (see figure 2)[2]. Given that free radical oxidation of arachidonic acid is believed to be a major source of γKAs in-vivo, and that free radicals can be regulated genetically this dissertation addresses the question whether the generation of γKAs can also be genetically regulated.

Figure 1

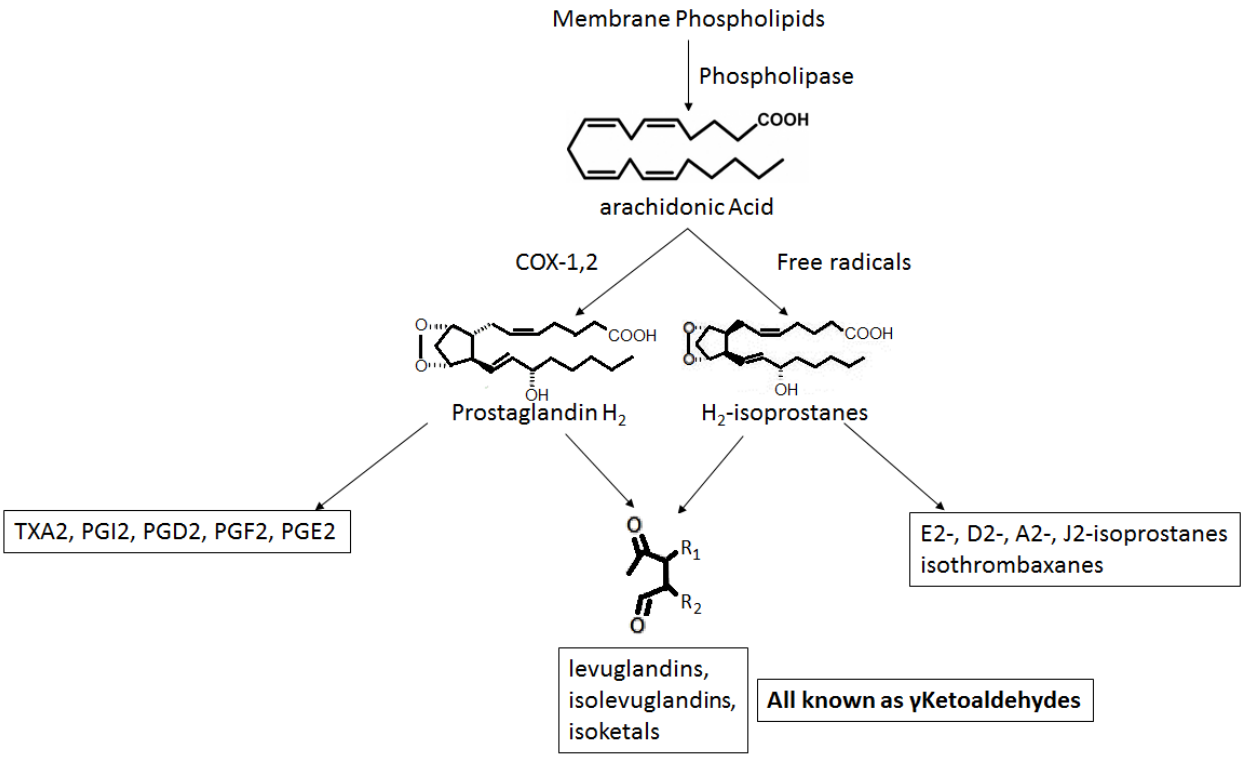

Figure 1: Generation of γKetoaldehydes

Figure 2

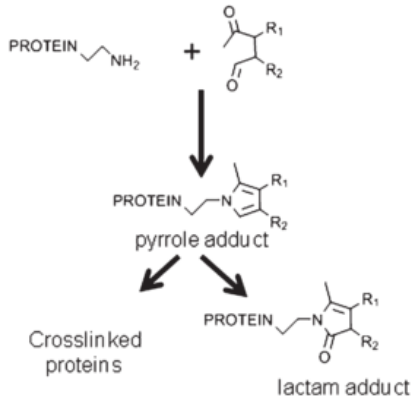

Figure 2: Mechanism of γKetoaldehydes binding to protein.
(adapted from Davies et al, JAD 2011)[2]

Oxidative Stress and its Regulation

Oxidative stress is defined as the imbalance in the equilibrium of reactive oxygen species (ROS) and antioxidant regulators[2]. Reactive oxygen species are comprised of but not limited to H_2O_2 (hydrogen peroxide), $\bullet O_2^-$ (superoxide anion) and •OH (hydroxyl radical)[7]. Reactive oxygen species can be generated by three major sources, including: the mitochondrial electron transport chain, the endoplasmic reticulum, and Nicotinamide adenine dinucleotide phosphate (NADPH) oxidases[8]. NADPH oxidases are transmembrane proteins located in multiple subcellular compartments (see figure 3)[9]. The main function of NADPH oxidase is to generate superoxide or hydrogen peroxide[10]. NADPH oxidases were historically discovered in phagocytes. This enzyme contains three cytosolic subunits ($p40^{phox}$, $p47^{phox}$, and $p67^{phox}$) and two membrane-bound subunits ($gp91^{phox}$ and $p22^{phox}$)[11]. Isoforms of NADPH oxidases Nox1, Nox2, Nox3, Nox4, Nox5, Duox1 and Duox2 can also be present in nonphagocytic cells[12]. Nox1, Nox2, Nox3, and Nox5 can generate superoxide, reducing oxygen by transporting

electrons across biological membranes and Duox1/2 and Nox4 can generate hydrogen peroxide directly (see figure 4)[7,12]. The generation of ROS by NADPH oxidases is involved in the induction of genes, ion transport, activation of transcription factors, and phosphorylation of kinases[4].

Antioxidants regulate the homeostasis of intracellular ROS. A master regulator of the antioxidant gene response is the transcription factor, nuclear factor erythroid 2-related factor 2 (NRF2) encoded by the nuclear factor erythroid-derived 2-like 2 (NFE2L2) gene. Under basal conditions cells quickly turnover Nrf2 via the ubiquitin-proteasome system (UPS), thus preventing the transcription of Nrf2 target-genes. This regulation is mediated through Kelch-like ECH-associated protein 1 (Keap1). Keap1 forms a dimer which recognizes Nrf2 through two key motifs located on the N-terminus of Nrf2[13,14]. When the Keap1 dimmer binds to these N-terminus domains of Nrf2, Nrf2 becomes polyubiquitylated and degraded by the proteasome[13].

When ROS levels are elevated Nrf2 becomes activated and translocates into the nucleus. Cysteine residues on Keap1 act as ROS sensors which become covalently modified by ROS or electrophilic molecules[15]. These modifications on Keap1 induce a conformational change which disrupts its binding to Nrf2 allowing for cytosolic Nrf2 to accumulate as it is no longer polyubiquitinated and degraded by the proteasome[16]. Cytosolic Nrf2 is then freely able to translocate into the nucleus and bind to antioxidant response elements (AREs) on DNA[17]. These DNA elements help transcribe crucial antioxidant genes such as glutamate-cytosine ligase catalytic subunit (GCLC), glutathione S-transferases (GSTs), heme oxidase (HO-1), superoxide dismutase (SOD), catalase (CAT), and NAD(P)H quinone oxidoreductase 1 (NQO1)[18,19]. Once ROS

homeostasis is restored, unmodified Keap1 can bind to Nrf2 and target it for polyubiquitination and proteosome degradation[20] (see figure 5).

Figure 3

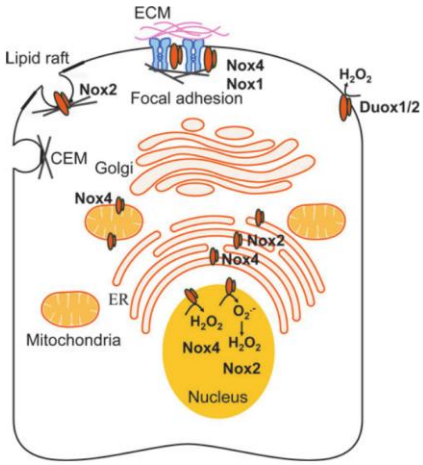

Figure 3: Subcellular localization of NADPH oxidases (Bernard et al., Antioxidants & Redox signaling, 2014)[9]

Figure 4

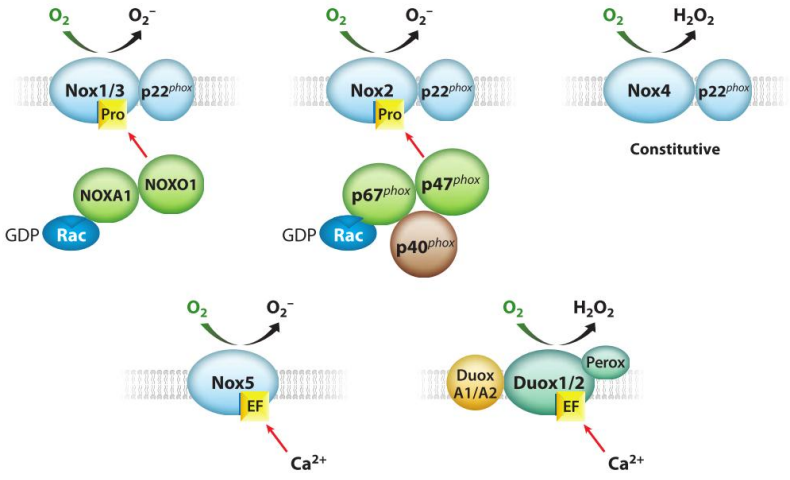

Figure 4: NADPH Oxidase Isoforms (Lambeth and Neish, Annual Reviews 2014)[12]

Figure 5

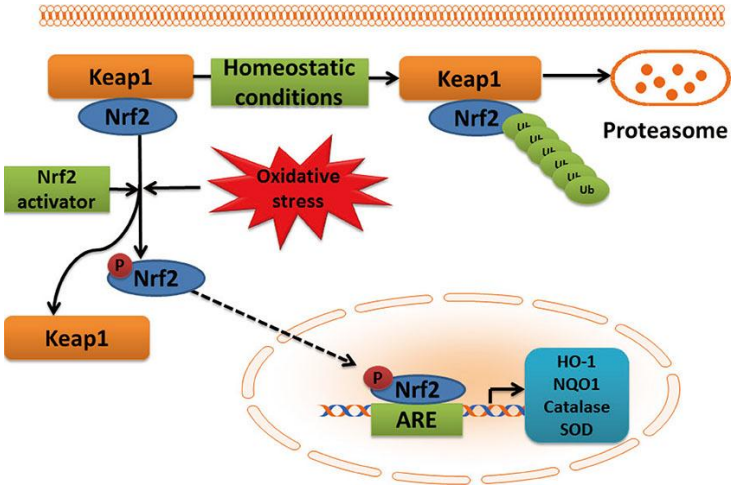

Figure 5: Nrf2 Gene Regulation

(Chen et al., Diabetes and Metaoblism, 2014)[20]

Role of NADPH Oxidases in the Lung

NADPH oxidase activity is present in several anatomical locations and in specific lung cells including, the lower and upper airways, and the gas-exchanging alveolar-capilary air sacs (see figure 6). Alveolar type I and type II epithelial cells comprise the alveolar epithelium. The epithelial sodium channel (Enac) has been shown to be crucial for lung function as it is expressed in type I and type II cells[21] and is responsible for alveolar gas exchange by regulating the clearance of alveolar fluid through Nox2 ROS production[22]. Nox2 and Nox4 play a role in pulmonary endothelial cells by in regulating inflammation, apoptosis, and vascular permeability[23]. The medial layer of the pulmonary vasculature is comprised of smooth muscle cells (SMCs). Nox4 is also involved in pulmonary SMCs and plays a role in the ability of SMCs to contract in response to inflammation[24,25].

Figure 6

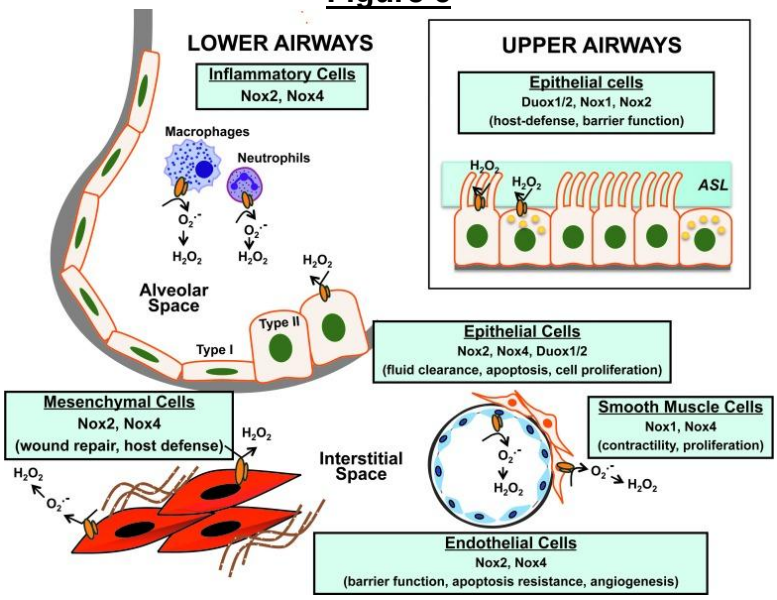

Figure 6: NADPH Oxidase Expression in the Lung (Bernard et al., Antioxidants & Redox Signaling, 2014)[9]

Oxidative Stress in Chronic Disease

Oxidative stress has been implicated in chronic diseases such as, cardiovascular disease, rheumatoid arthritis, neurodegenerative and neurological diseases, kidney disease, cancer, ocular disease, and pulmonary disease. For cardiovascular disease, oxidative stress has been implicated in ischemia, hypertension, cardiomyopathy, atherosclerosis, congestive heart failure, and cardiac hypertrophy[26–28]. In rheumatoid arthritis the synovial fluid around joints has been shown to contain increased levels of prostaglandins and isoprostanes[29]. Additionally rheumatoid arthritis is a disease which is known for its chronic inflammation around joints caused by infiltrating T-cells and macrophages[30,31]. Neurodegenerative and neurological diseases, such as Parkinson's disease, Alzheimer's disease, amyotrophic lateral sclerosis (ALS), multiple sclerosis, and depression have all been associated with oxidative stress[32–35]. Chronic oxidative

stress has also been shown to play a role in renal diseases such as uremia, chronic renal failure, glomerulonephritis, tubulointerstitial nephritis, and proteinuria[36–38]. Oxidative stress has also been demonstrated in ocular diseases have such as cataracts and age-related macular degeneration[38–41]. Lastly and of particular focus of this dissertation, oxidative stress has also been shown to play a role in pulmonary diseases such as, pulmonary fibrosis, as well as asthma and chronic obstructive pulmonary disease (COPD)[42–46]. In summary the study of oxidative stress has a broad impact on several chronic diseases.

Pathogenesis and Murine Models of Pulmonary Fibrosis

Pulmonary fibrosis is known to be a chronic lung disease characterized by an excessive accumulation of extracellular matrix (ECM) leading to remodeling of lung architecture. It was originally diagnosed through recognizable physiologic, radiographic and clinical findings. Historic descriptions of pulmonary fibrosis have been documented as early as the 5th century BC by Hippocrates[47,48]. Modern descriptions of this disease began to occur in the early 20th century[49,50]. Currently, idiopathic pulmonary fibrosis (IPF) is considered the most common and most severe form of pulmonary fibrosis. In a recent study, the prevalence of IPF was 41.8 per 100,000 people with an incidence rate of 18.7 per 100,000[51]. The average age at diagnosis is 66 years[52,53]. IPF has a median survival of approximately three years, with no proven effective therapy[53,54]. Lung transplantation remains to be the only viable intervention in end-stage disease[55].

The lung has evolved to contain specialized fluid which lines the epithelium containing antioxidants to aid with maintaining basal levels of reactive oxygen species

(ROS)[56]. In disease states involving ROS, this line of defense can be overwhelmed and has been associated with the pathogenesis of IPF[53]. The onset of IPF is thought to be much earlier in life given that most patients have severe pulmonary disease at the time of clinical presentation[52,53]. IPF is thought to be a result of chronic and unresolved fibrotic scaring of the lung. Tissue scaring is known to be initiated by an influx of inflammatory cells. Neutrophilia is present in 70-90% of IPF cases, while 40-60% present with eosinophilia in bronchoalveolar lavage fluid[57] which play a role in increased mortality[58–61]. Inflammatory cells have also been shown to play a role in fibrosis models[62]. These observations have been the basis for the rationale to treat IPF patients with anti-inflammatory drugs[53,63]. However this treatment has failed in the clinic[64–66] and the current prognosis for IPF patients is poor, with a mean time of survival of approximately 3 years after diagnosis[53,54]. Fibrosis has also been characterized by fibroblast differentiation into myofibroblasts, epithelial to mesenchymal transition also contributing to myofibroblast differentiation, and the accumulation of extracellular matrix (ECM) contributing to tissue stiffness[9,67–72]. Tissue stiffness has been associated with the generation of reactive oxygen species by lung myofibroblasts by inducing ECM crosslinking reactions[73]. In addition, the $p47^{phox}$ subunit of Nox2 has been shown to be required for pulmonary fibrosis development in murine models[9,62]. Nox4 has also been shown to be involved in the progression of fibrosis and its inhibition has been demonstrated to be an effective treatment in mouse models[74].

There are several murine models of pulmonary fibrosis used today. These models help serve as tools to aid in the investigation of new therapeutic treatments as well as aid in the understanding of the initiation and progression of pulmonary fibrosis.

Current mouse models[75] used are: Bleomycin induced fibrosis, Silica induced fibrosis, FITC (fluorescein isothiocyanate) induced fibrosis, adoptive cell transfer, transgenic models using pulmonary-specific transgenes or viral-targeted transgene delivery, and of particular focus in this dissertation irradiation-induced fibrosis. The bleomycin model is one of the most studied models of pulmonary fibrosis. Bleomycin is an antibiotic originally discovered and isolated from *Streptomyces verticillatus*[76]. Bleomycin has been used to treat skin tumors such as squamous cell carcinomas[77] but its toxicity in regards to promoting pulmonary fibrosis resulted in limiting the use of this drug[78]. Bleomycin can induce lung toxicity by intravenous (iv), intraperitoneal (ip), intratracheal (it), or subcutaneous (sc) delivery in several species including, mice, hamsters, rats, guinea pigs, rabbits, dogs, and primates[78]. Epithelial damage is believed to be the initial injury caused by bleomycin[79]. Acute lung injury caused by bleomycin causes hyaline membrane formation, alveolar consolidation and leakage of plasma proteins into the alveolar space[78]. Bleomycin induces a focal necrosis of type I and type II alveolar epithelial cells along with an infiltration of inflammatory cells[79,80]. Inflammatory cells are subsequently cleared and proliferation of myofibroblasts contribute to the production of extracellular matrix[81]. Fibrosis develops at around 14 days in this model with peak accumulation of fibrosis between days 21-28[81–84]. This model of pulmonary fibrosis however is not chronic and some reports show a resolution of fibrosis between 60-90 days of bleomycin treatment[84,85]. Compared to the bleomycin model of pulmonary fibrosis, radiation-induced lung fibrosis has been shown to induce a chronic state of injury leading to death[86]. The model of radiation-induced pulmonary fibrosis is dependent on murine genetic background and irradiation dose. The CBA/J and

C3H/HeJ mouse strains are fibrosis resistant[87,88]. Thoracic radiation treatment to these strains develop radiation-induced pneumonitis[87,88]. In contrast the C57Bl/6J strain respond with developing late onset pulmonary fibrosis after thoracic radiation[87,88]. After 33 weeks of a thoracic dose of 16 Gy results in subpleural foci of damaged alveolar walls along with collagen deposition, in the C57Bl/6J background[89]. Reports have also shown that in this model, macrophages and fibroblasts accumulate in fibrotic foci[90]. Protection of radiation-induced fibrosis has been reported through intratracheal delivery of manganese superoxide dismutase-plasmid/liposomes 24 h before lung irradiation[90].

CHAPTER II

MATERIALS AND METHODS

Cell Culture

Human microvascular endothelial cells (HMVECs), murine 3B11 endothelial cells, and murine alveolar type II MLE12 cells were obtained from ATCC and grown according to ATCC recommendations. Exponentially growing 3B11 cells were administered 5 Gy at room temperature using a Cesium-137 irradiator (2 Gy/min; JL Shepherd, Mark 1) and then incubated at 37°C for 24 hours before harvesting. HMVECs were treated with 150 μM H_2O_2 in PBS for 1 hr at 37°C, washed extensively, and incubated at 37°C for 24 hours before harvesting.

Mice

Congenic C57BL/6J mice with a targeted disruption of the Nfe2l2 gene have been described previously[86]. Mice were X-irradiated between 7 and 10 months of age[86]. Mice were maintained under specific pathogen free conditions. All procedures performed on animals were approved by the Institutional Animal Care and Use Committee at Vanderbilt University and at the University of Texas MD Anderson Cancer Center, and complied with all state, federal, and NIH regulations.

Congenic C57BL/6J mice harboring a targeted disruption of the Ncf1 gene have been described previously[91]. Mice were bred and maintained under specific pathogen free conditions at the animal care facility at Roswell Park Cancer Institute, Buffalo, NY. Mice were 8-15 weeks of age. All procedures performed on animals were approved by

the Institutional Animal Care and Use Committee at Roswell Park Cancer Institute and complied with all state, federal, and NIH regulations.

Immunohistochemistry

Paraffin-embedded lung tissue (5 µm) were prepared at the Mouse Pathology Core Facility at Vanderbilt University. H&E stains were performed using standard protocols. Lung tissue sections were incubated with primary antibody overnight at 4°C. Sections without primary antibody served as negative controls. Nitro-blue tetrazolium chloride (NBT) and 5-bromo-4-chloro-3'-indolyphosphate p-toluidine salt (BCIP, catalog no. 34070, Thermo Fisher Scientific) were used to produce localized visible staining. Slides were counterstained with methyl green. IHC stained IPF tissues were independently and blindly assessed for positive staining by Vanderbilt Idiopathic Pulmonary Fibrosis Center personnel.

Imunnofluorescence staining (IF)

Mouse lungs were perfused with phosphate buffered saline, pH 7.2 (PBS) through the pulmonary artery and fixed with 10% phosphate-buffered formalin. After fixation lungs were processed and paraffin-embedded. Paraffin-embedded lung tissue was sectioned into 5µm slices and mounted on glass slides.

The following primary antibodies were used: single chain ScFv anti-γKA antibody, (D11, 1:100 dilution, see (Davies et al[92] for details of preparation), Goat polyclonal anti-SPC antibody (catalog no. sc-7706, 1:100 dilution; Santa Cruz), Goat polyclonal anti-T1α Podoplanin antibody (catalog no. sc-23564, 1:100 dilution; Santa

Cruz), Rabbit polyclonal anti-CC10 antibody (catalog no. sc-25555, 1: 100 dilution; Santa Cruz), Goat polyclonal anti-PECAM-1 antibody (catalog no. sc-1506, 1:100 dilution; Santa Cruz), Goat polyclonal anti-COL1A1 antibody (catalog no. sc-8784, 1:100 dilution; Santa Cruz). Of note, D11 ScFv recognizes peptides and proteins modified on the lysine residues by γKA isomers that arise from both the free radical and cyclooxygenase pathway and recognition is not dependent on amino acids adjacent to the modified lysine[92]. The D11 ScFv encodes the E-tag sequence used for detection. After primary antibody incubation, lung sections were washed in PBS. A secondary antibody raised against the E-tag epitope was then used to detect D11 binding. Anti-E-tag antibody was diluted in 10% BSA and sections were incubated 1hr at RT. Rabbit polyclonal anti-E-tag antibody (catalog no. ab3397, 1:1,000 dilution; Abcam), was used for dual-stained with goat-raised primary antibodies; Goat polyclonal anti-E-tag antibody (catalog no. ab95868, 1:1,000 dilution; Abcam) was used for dual-stained with rabbit raised primary antibodies. After anti-E-tag antibody incubation sections were washed in PBS. Sections were then incubated with fluorescently tagged antibodies diluted in 10% BSA for 1hr at RT. The following fluorescently tagged antibodies were used sequentially: Donkey Anti-Goat Alexa 647 (catalog no. A-21447, 1:1,000 dilution; Life Technologies) and Goat Anti-Rabbit Alexa 568 (catalog no. A-11011, 1:1,000 dilution; Life Technologies). After incubation with fluorescently tagged antibodies sections were then washed in PBS and mounted with ProLong Gold Antifade Mountant with DAPI (catalog no. P36931, Life Technologies) and sealed with glass coverslips. For specificity controls, primary antibody was not added.

Imunnofluorescence Image Acquisition

Confocal images were acquired using an Olympus FV-1000 inverted confocal microscope provided by the VUMC Cell Imaging Shared Resource. Z-stack images were taken at 0.45um slice thickness using a 60x / 1.45 Plan-Apochromat oil immersion objective lens. Wide-field immunofluorescence images were acquired using a Leica DM IRB inverted microscope equipped with a Nikon DXM1200C camera provided by the IMSD program at Vanderbilt.

Immunofluorescence Intensity Quantification

The following steps were taken to quantify pixel intensity. Each 16 bit image obtained when primary (ie. D11) and secondary antibody was used was opened in ImageJ. The threshold function was used to highlight immunofluorescence and to identify a representative threshold. This representative threshold was then applied to every image obtained when primary and secondary antibody was used. This same representative threshold was used for all images obtained when secondary alone was used. All threshold images were then converted to binary. A mean integrated density (defined as the sum of the value of the pixels in the image) $\pm$ SD was determined for primary/secondary antibody and for secondary antibody alone.

DAPI staining for each image was quantified using the percent area fraction in ImageJ. Area fraction is defined in ImageJ as the percentage of non-zero pixels per field. The mean area fraction for DAPI staining $\pm$ SD was calculated for each image. The mean integrated density of each image was divided by its corresponding area fraction (ie DAPI staining) to correct for tissue cellularity. A non-parametric Mann

Whitney test was used to determine if primary antibody yielded immunofluorescence/DAPI staining that was significantly more intense than secondary alone. An example is shown below. In this example secondary alone (negative control) encompasses immunofluorescence produced by secondary antibodies composed of rabbit anti-E tag antibody and anti-rabbit Alexa 568, as well as tissue auto-fluorescence. D11-specific immunofluorescence is 10.3 fold above negative control mean immunofluorescence ($P = 2.39 \times 10^{-21}$, N = 10 fields, 100 Z stack images).

Image J quantification using Threshold Function

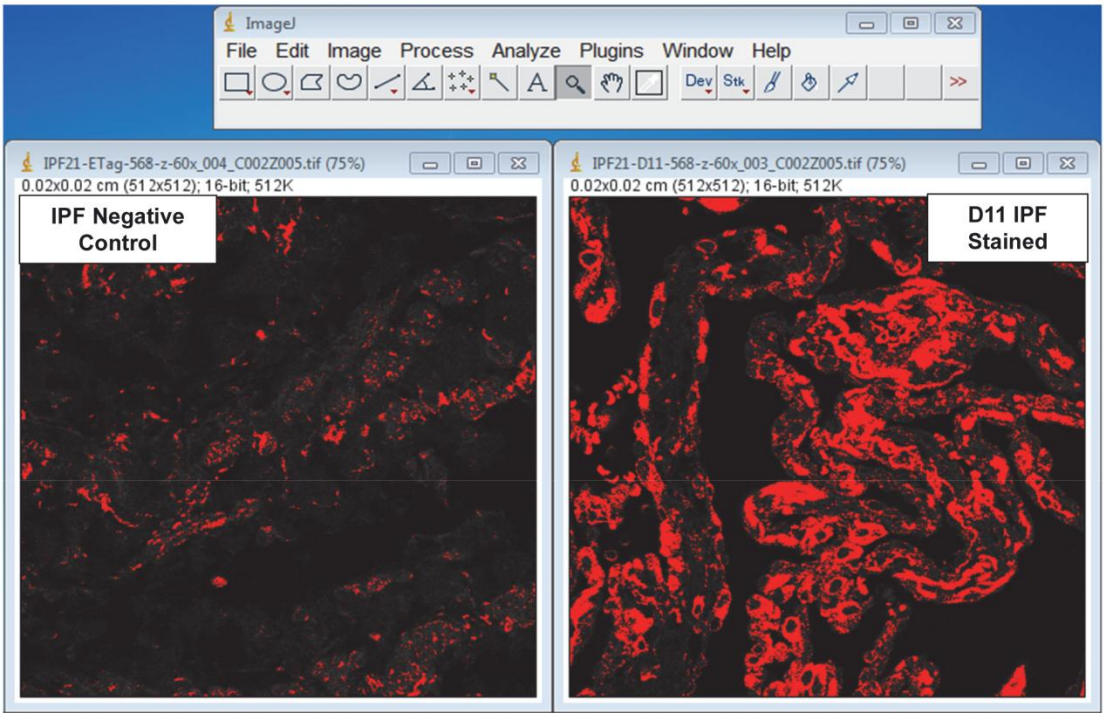

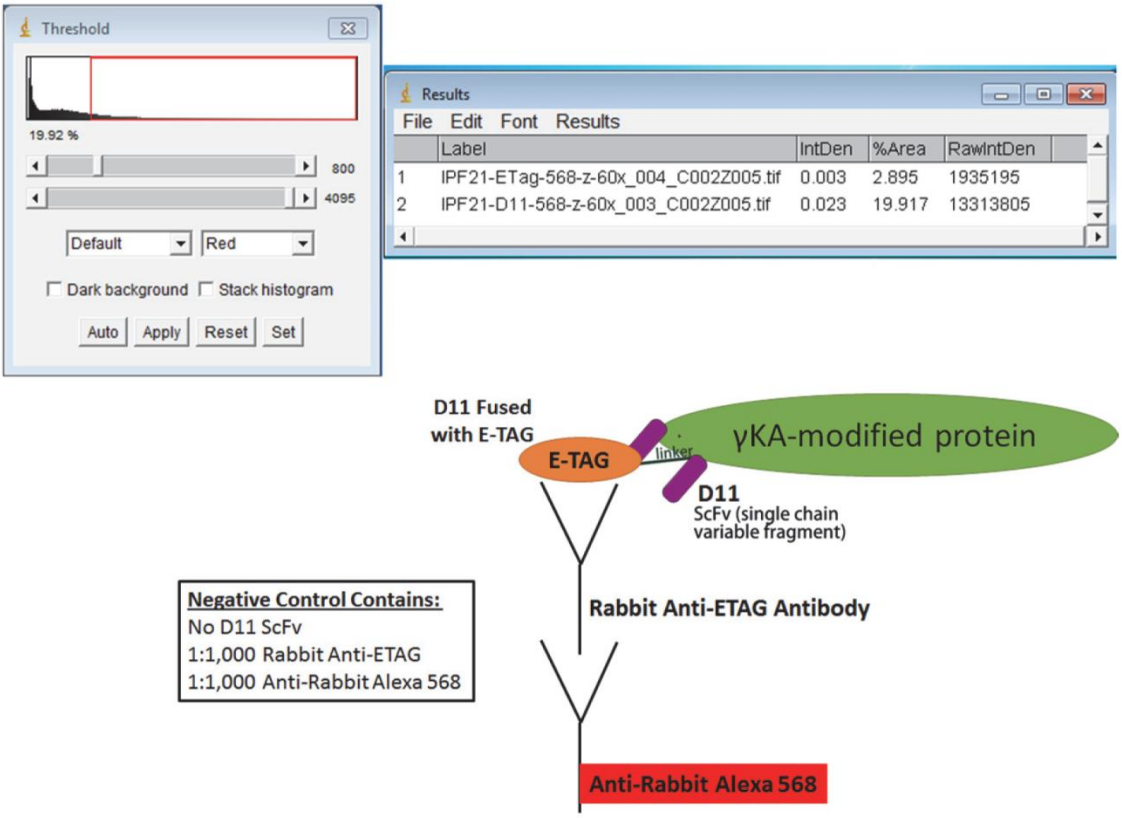

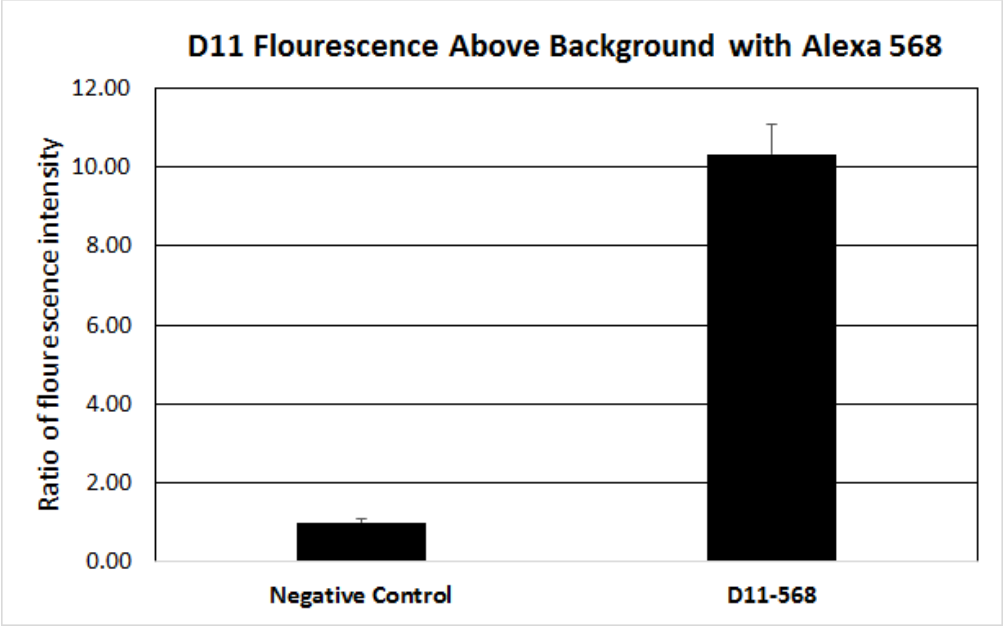

The above figure illustrates the mean ratio of fluorescence intensity (immunofluorescence from images (N = 10 fields with 10 z stack images) obtained when

negative control (define above) and primary D11-specific immunofluorescence was quantified.

Immuno-affinity Isolation of γKA-modified proteins

Cells were lysed in 0.1% NP40-PBS, pH 7.2 and the lysate centrifuged at 12,000 xg for 10 min. The supernatant was adjusted to 0.1%, NP40, 0.1% SDS, in PBS, pH 7.2. Proteins were extracted from the pellet using 500mM NaCl-PBS, pH 7.2, brought to isotonic conditions (100mM NaCl with 0.1%, NP40, 0.1% SDS, in PBS, pH 7.2), sonicated on ice, and then centrifuged at 12,000xg for 10 min. The resulting supernatant was recovered.

Soluble protein was precleared using protein A/G beads. Ten ug D11 ScFv was used to isolate γKA-modified proteins (16 hrs/4°C). Anti-E-tag antibody conjugated agarose beads (catalog no. ab19368; Abcam) were used to capture D11 ScFv antibody. Beads were subsequently washed with 0.1% NP40, 0.1% SDS, in PBS pH7.2. Purified proteins were solubilized in 5X loading buffer and boiled for 7mins, resolved approximately 3 cm on an SDS-PAGE gel, stained with coomassie blue and the entire lane excised for LC-MS/MS analysis.

As a control for D11 ScFv specificity the following reactions were performed: 500uM 4-hydroxynonenal (HNE) was reacted with 5mM lysine for 24hrs at RT. Unreacted HNE was quenched using 50mM Tris-HCl. 10 µg D11 ScFv was added to HNE-Lysine complex and incubated overnight at 4°C prior to being used for immunoprecipitation of γKA-modified proteins.

LC-MS/MS Analysis of Affinity Purified Proteins

D11 immunoaffinity purified proteins from sham and irradiated 3B11 cells were subjected to in-gel trypsin digestion and the resulting peptides analyzed by a 70 minute data dependent LC-MS/MS run. Briefly, peptides were auto--sampled onto a 200 mm by 0.1 mm (Jupiter 3 micron, 300A), self-packed analytical column coupled directly to an LTQ (ThermoFisher) linear ion trap mass spectrometer via a nanoelectrospray source and resolved using an aqueous to organic gradient. A series in which a full scan mass spectrum (MS) followed by 5 data-dependent tandem mass spectra (MS/MS) was collected throughout the run with dynamic exclusion enabled to minimize acquisition of redundant spectra. MS/MS spectra were searched via SEQUEST a mouse protein database (UniprotKB) that also contained reversed version for each of the entries. Spectral identifications were filtered and collated into spectral count numbers at the protein level using Scaffold (Proteome Software).

Histone Isolation from Tissue

Histone isolation was performed as described[93]. Isolated murine lung tissue was lysed in hypotonic lysis buffer (10mM HEPES/KOH pH=7.9, 1.5mM MgCl2, 10mM KCl, 5mM Sodium Butyrate, 0.5% NP-40, with protease and phosphatase inhibitors). Nuclei was then isolated by centrifugation (4,000 rpm for 10 minutes at 4°C) and washed with hypotonic lysis buffer. Nuclei pellet was then resuspended in high salt buffer (20mM HEPES/KOH pH=7.9, 1.5mM MgCl2, 420mM KCl, 0.2mM EDTA, 25% Glycerol, 5mM Sodium Butyrate, with protease and phosphatase inhibitors) and sonicated. This high salt suspension was rotated at 4°C for 18 hours. Chromatin was later pelleted and

isolated by centrifugation (4,000 rpm for 20 minutes at 4°C). Pellet containing histone proteins (as evidence by coomassie blue staining, see figure 12) was resuspended in low salt buffer (20mM HEPES/KOH pH=7.9, 1.5mM MgCl2, 0.2mM EDTA, 5mM Sodium Butyrate, with protease and phosphatase inhibitors).

Human Idiopathic Pulmonary Fibrosis and Organ Donor Lung Tissue

Collection, storage of samples and experimental protocols were carried out in accordance with relevant guidelines and regulations approved by the Vanderbilt University Institutional Review Boards (Vanderbilt IRB Protocol 9401). Written informed consent was obtained from all subjects. Human tissue sections were obtained from explanted IPF lungs at the time of transplant. Control tissue was obtained from lungs rejected for organ donation at Vanderbilt University. IPF diagnosis was confirmed by multidisciplinary review according to the 2011 ATS/ERS Consensus Guidelines[55].

Measurement of Apoptosis

Percent of apoptosis was measured using the Annexin V-fluorescein isothiocyanate apoptosis detection kit I (Pharmingen) with flow cytometry according to the manufacturer's directions.

MMP-1 degradation assay with Collagen 1α1

Purified human recombinant Collagen 1α1 was incubated with purified γKA at 37°C/1hr, after which unreacted γKA was quenched. MMP1 was the added to the

reaction and incubated at 37°C/0.5hr, pH = 7.0. Col1α1 degradation was analyzed by 1D SDS PAGE, Coomassie Blue staining.

Statistical Analysis

An unpaired t test or an analysis of variance was used for comparison between various groups. A P value less than 0.05 was considered as statistically significant.

CHAPTER III

CELL TYPES WHICH HARBOR γKA-MODIFIED PROTEIN IN LUNG TISSUE

Results:

γKA-modified protein are present in murine lung tissue. To determine the lung cell types which harbor γKA-modified protein murine lung samples were obtained from non-diseased C57BL/6J mice maintained under stress-free conditions and continuous access to water, food and regular 12hr light cycles. Lung tissue sections underwent dual-immunofluorescence staining for γKA-modified proteins, and Type 2 alveolar epithelial cells, Type 1 alveolar epithelial cells, Club cells, or endothelial cells. γKA-modified proteins were identified using the well characterized single chain antibody D11 ScFv, which recognizes peptides and proteins modified by γKA isomers that can arise from both the free radical and cyclooxygenase mediated pathways[92,94–96]. γKA-modified protein was observed in each cell type, suggesting that the burden of γKA-modified protein is a byproduct of normal lung metabolism (see figure 7).

γKA-modified protein are present in human lung tissue. Having shown that γKA-modified proteins are present in mouse lung, whether human lung also exhibited a basal level of γKA modification was investigated. Formalin-fixed paraffin-embedded (FFPE) pulmonary tissue obtained from 2 control organ donors (see table 1 subjects 5 and 6) underwent IHC staining with the D11 antibody, counterstained with methyl green and imaged by wide field microscopy (see figure 8). Very little D11 immunoreactivity was noted. Next, confocal microscopy was used to image FFPE tissue immunostained with

D11 and counter stained using DAPI. The confocal images illustrate the presence of a low level of γKA-modified protein in human lung tissue (see figure 8), confirming the observations of others[96] suggesting that human lung tissue can have a basal level of γKA-modified protein.

Figure 7

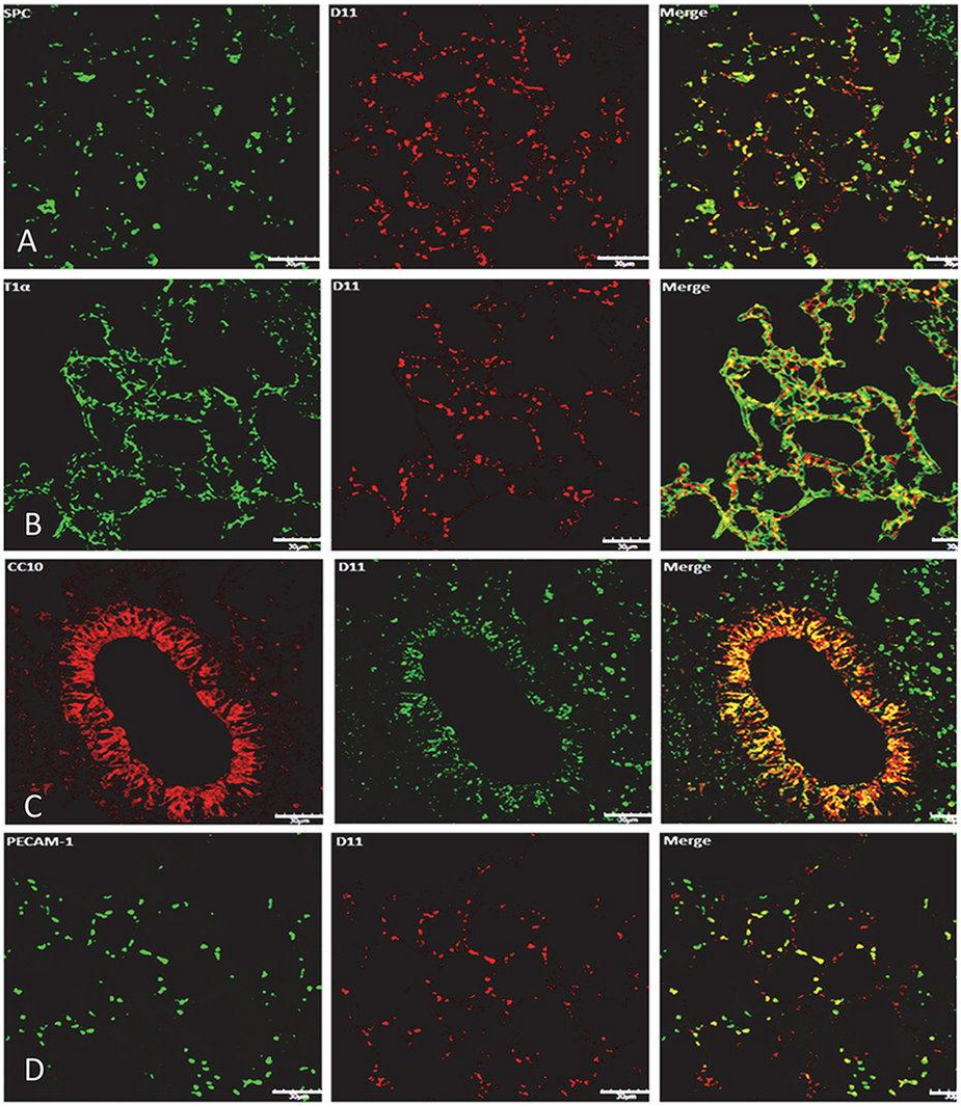

Figure 7: γKA-modified protein are present in several cell types in murine lung tissue. Mouse lung tissue sections were immunostained with the following: (A) anti-SPC for Type 2 alveolar cells (Alexa 647 secondary, green false color), D11 ScFv (Rhodamine Red secondary); (B) anti T1α for Type 1 alveolar cells (Alexa 647 secondary, green false color), D11 ScFv (Rhodamine Red, secondary); (C) anti-CC10 for Club cells (Rhodamine Red secondary), D11 ScFv (Alexa 647 secondary, green false color); (D)

anti-PECAM-1 for endothelial cells (Alexa 647 secondary, green false color), D11 ScFv (Rhodamine Red secondary). Images were acquired using confocal microscopy (60× magnification). The white bar represents 30 μm. (Mont S. et al, Sci Reports 2016)[97]

Table 1

Patient Characteristics

Subject Number	Age	Gender	Diagnosis	Race/Ethicity	Tobacco Use	Pack Years	FVC%
1	67	Female	IPF	Caucasian	Yes	90	68
2	67	Male	IPF	Caucasian	Yes	42	82
3	61	Male	IPF	Caucasian	Yes	15	51
4	59	Female	Control	Caucasian	Yes	Unknown	Unknown
5	52	Female	Control	Caucasian	Unknown	Unknown	Unknown
6	32	Female	Control	Caucasian	No	NA	Unknown

Table 1: Patient characteristics of human lung samples. (Mont S. et al, Sci Reports 2016)[97]

Figure 8

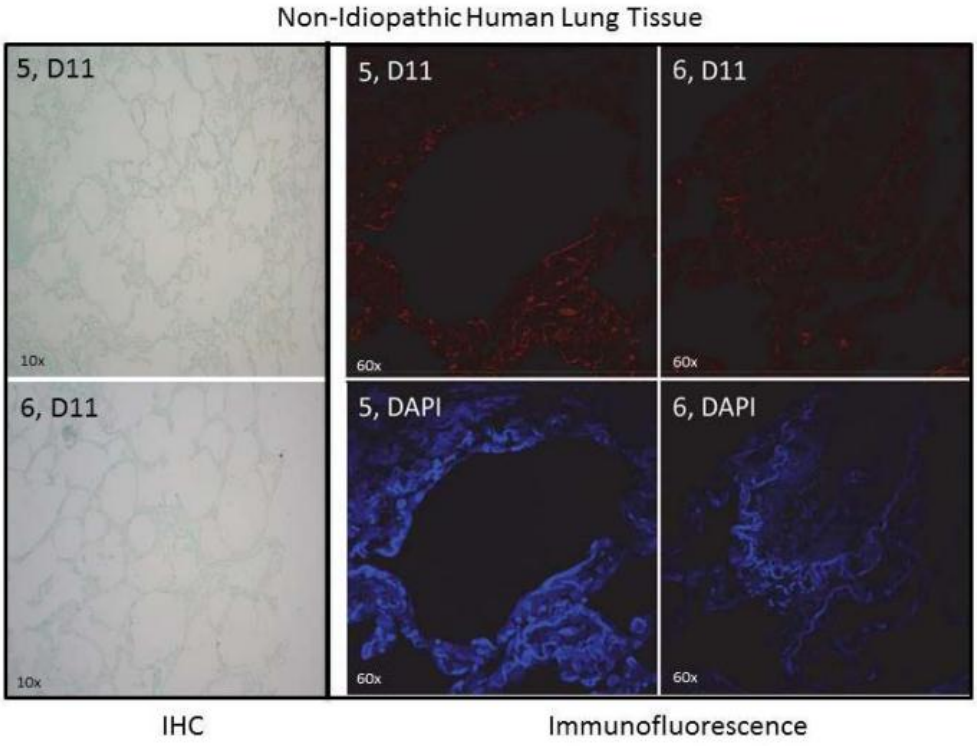

Figure 8: Human lung tissue sections stained for γKA-modified proteins. Human lung tissue sections from organ donors 5 and 6 underwent IHC staining with the D11 antibody, counterstained with methyl green and imaged using wide field microscopy or were immunostained with D11 (Red), counterstained with DAPI (blue) and imaged by confocal microscopy. (Mont S. et al, Sci Reports 2016)[97]

CHAPTER IV

GENETIC REGULATION OF γKA FORMATION AND PROTEINS WHICH ARE SUSCEPTIBLE TO γKA MODIFICATION

Results:

NADPH oxidase promotes generation of γKA-modified protein. To determine if γKA-modified proteins could be genetically regulated by cellular superoxide, pulmonary tissue was obtained from age-matched $p47^{phox}$ null and wild type C57BL/6J mice. $p47^{phox}$ is an activating subunit of Nox2, and is a major source of cellular superoxide[98]. Quantification of γKA-modified protein by D11 immuno-reactivity using immunofluorescent/DAPI staining in pulmonary tissue obtained from $p47^{phox}$ null mice demonstrated a 55% ($P = 0.006$) loss of γKA-modified protein. This data suggests that Nox2 is a major source for the generation of γKA-modified protein in murine lung tissue (see figure 9).

Nrf2 suppresses generation of γKA-modified protein. The Nrf2-null mouse represents a well characterized model for investigating ROS interactions[86]. Pulmonary tissue was obtained from Nrf2-null and age-matched wild type C57BL/6J mice. Quantification of γKA-modified protein by D11 immuno-reactivity using immunofluorescent/DAPI staining in pulmonary tissue obtained from wild type and Nrf2-null mice revealed that loss of Nrf2 resulted in a 2-fold increase in γKA-modified protein ($P = 0.003$). Taken together, these data show that genes regulating oxidative stress can substantially alter accumulation of γKA-modified protein (see figure 10).

LC-MS analysis of immuno-affinity purified γKA-modified proteins. Currently, there is little knowledge concerning the identity of proteins that are susceptible to γKA modification. Endothelial cells were chosen to identify proteins adducted endogenously due to their well characterized and robust NADPH oxidase activity[99]. γKA-modified proteins from 3B11 endothelial cells were immuno-affinity purified using the D11 antibody. Proteins were subjected to LC/MS/MS analysis. Analysis of 3 independent experiments identified 162 proteins. A PANTHER network and pathway analysis[100] of Molecular Function was performed which revealed that proteins susceptible to adduction are not restricted to an organelle or class of proteins, but can be classified into several distinct cellular pathways (see figure 11 and database table published by Mont S. et al, Scientific Reports, 2016: *Supplementary Table S1*)[97]. In addition, γKA-modified proteins were immuno-affinity purified from 3B11 cells 24 hrs after administering 5 Gy. Isolated proteins were again subjected to LC/MS/MS. Ninety four percent of the proteins identified in the irradiated samples were also found in sham treated samples. Proteins specific to the irradiated samples are noted in red font, (see database table published by Mont S. et al, Scientific Reports, 2016: *Supplementary Table S2*)[97]. Based on the observations that there was a 2 fold increase in D11 immunoreactivity in irradiated cells compared to sham (see figure 13 in Chapter 5) the current hypothesis is that cells contain a 'pool' of susceptible γKA-modified proteins, with the fraction of proteins modified within the pool increasing as oxidant stress increases.

Confirmation of γKA-modified histone-H3 and histone-H4. Histones have been shown to be susceptible to modification by reactive lipid electrophiles, including γKAs (specifically levuglandin E2) and 4-oxononenal, resulting in stable lysine adducts[93,101]. Mass spectrometry analysis demonstrated the presence of histone H4, H1.3, H1.4, H2A, H2B, and H3.3 peptide profiles detected by mass spectrometry following D11-mediated purification (see database table published by Mont S. et al, Scientific Reports, 2016: *Supplementary Table S2,* tab Binding)[97]. γKA-histone modification was measured by isolating chromatin from mouse whole lung homogenates[93]. Immunoblotting of chromatin with D11 confirmed the modification of histones H3 and H4 in mouse lung tissue (see figure 12).

Figure 9

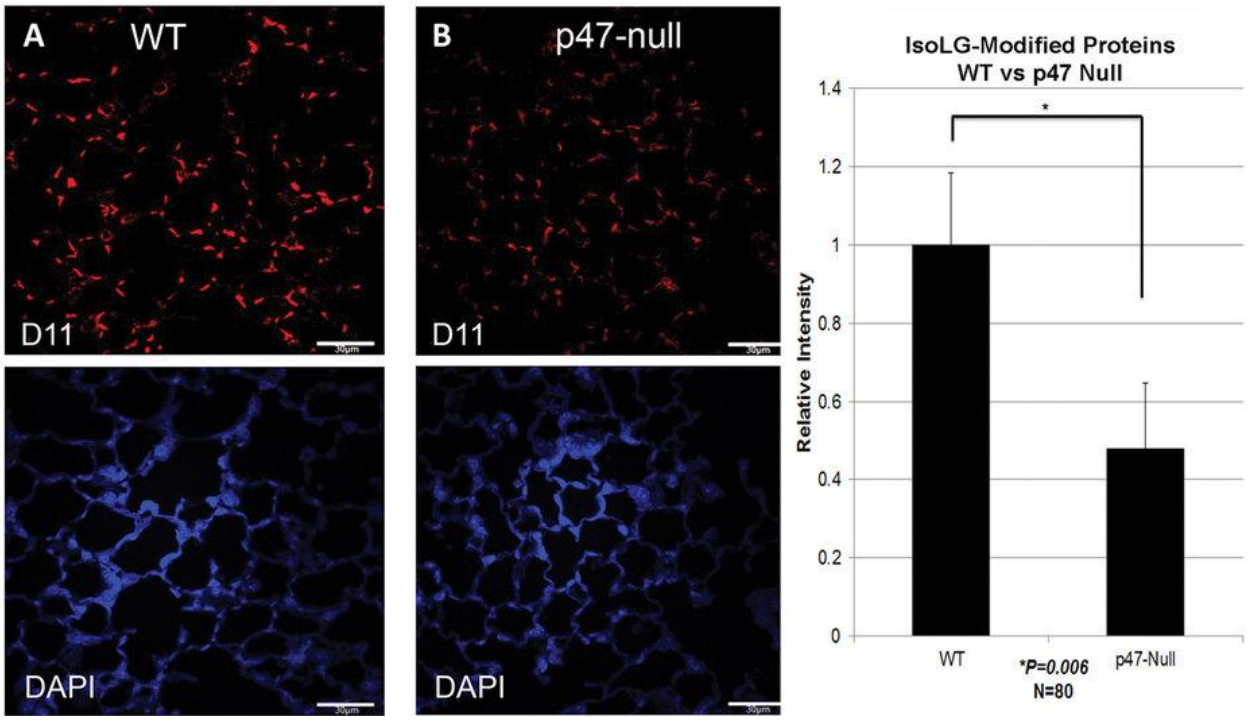

Figure 9: NADPH oxidase promotes generation of γKA-modified protein. IsoLG-modified protein in formalin fixed paraffin embedded pulmonary tissue from age matched wild type (A and C, N = 6) or p47^{phox} null (B, N = 3). Images were acquired using confocal microscopy (60× magnification). Quantification of D11 ScFv immunofluorescence,

corrected for DAPI staining is shown on the right for p47 phox null vs wild type (N = 80 random fields). White bars represents 30 µm. (Mont S. et al, Sci Reports 2016)[97]

Figure 10

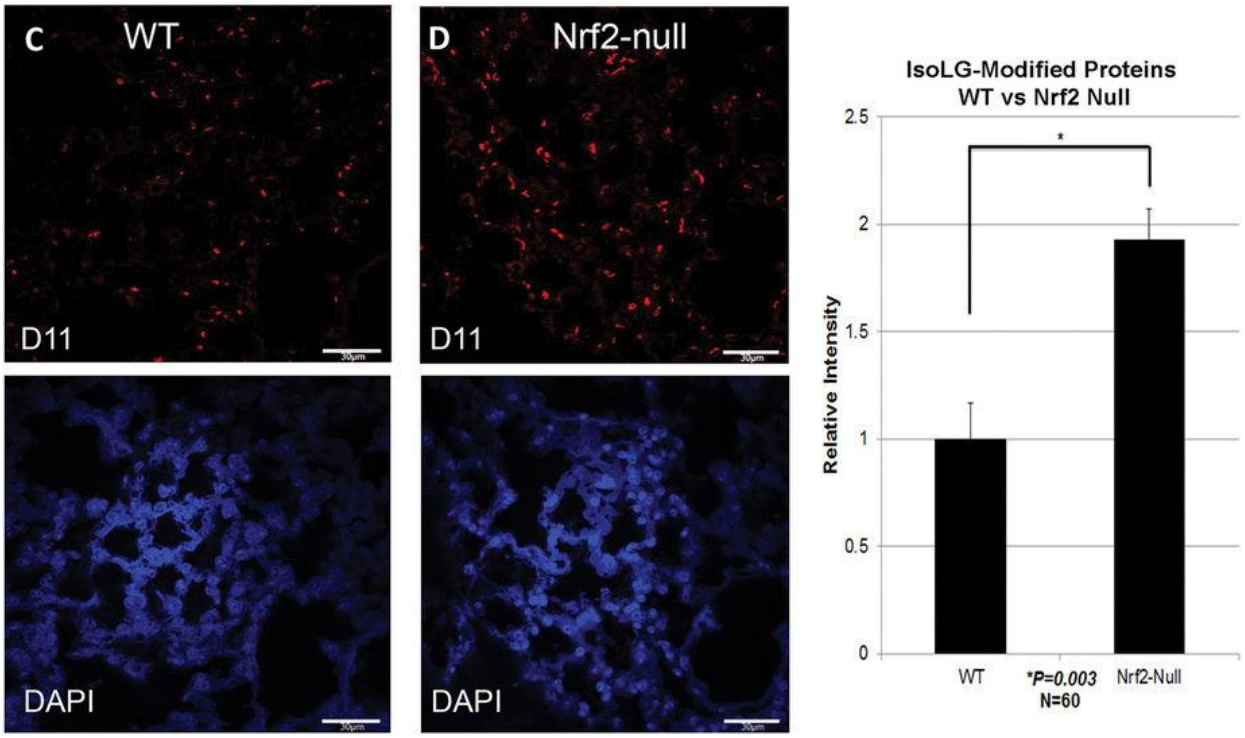

Figure 10: Nrf2 suppresses generation of γKA-modified protein. IsoLG-modified protein in formalin fixed paraffin embedded pulmonary tissue from age matched wild type (A and C, N = 6) or Nrf2 null (B, N = 3). Images were acquired using confocal microscopy (60× magnification). Quantification of D11 ScFv immunofluorescence, corrected for DAPI staining is shown on the right for Nrf2 null vs wild type (N = 60 random fields). White bars represents 30 µm. (Mont S. et al, Sci Reports 2016)[97]

Figure 11

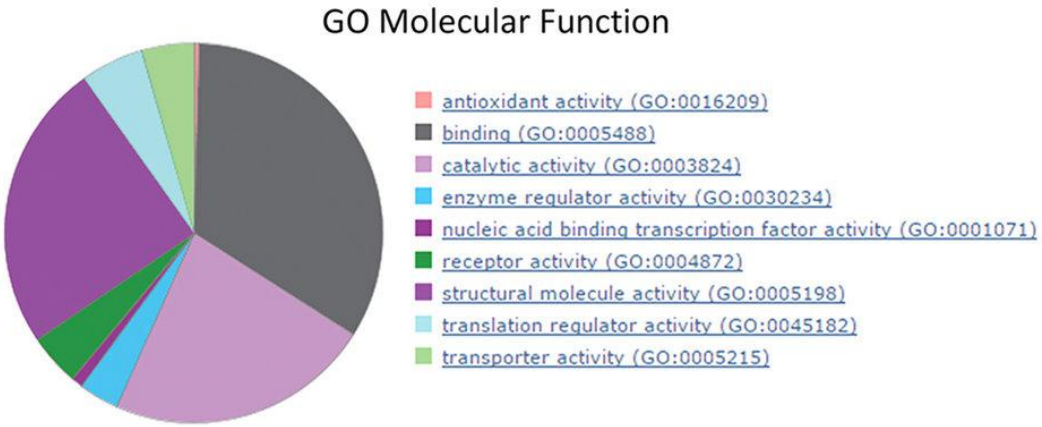

Figure 11: PANTHER analysis of endogenous γKA-modified proteins. Protein lysates from mouse 3B11 endothelial cells were immunoprecipitated with D11 ScFv, subjected to LC/MS/MS and then analyzed using the PANTHER software. (Mont S. et al, Sci Reports 2016)[97]

Figure 12

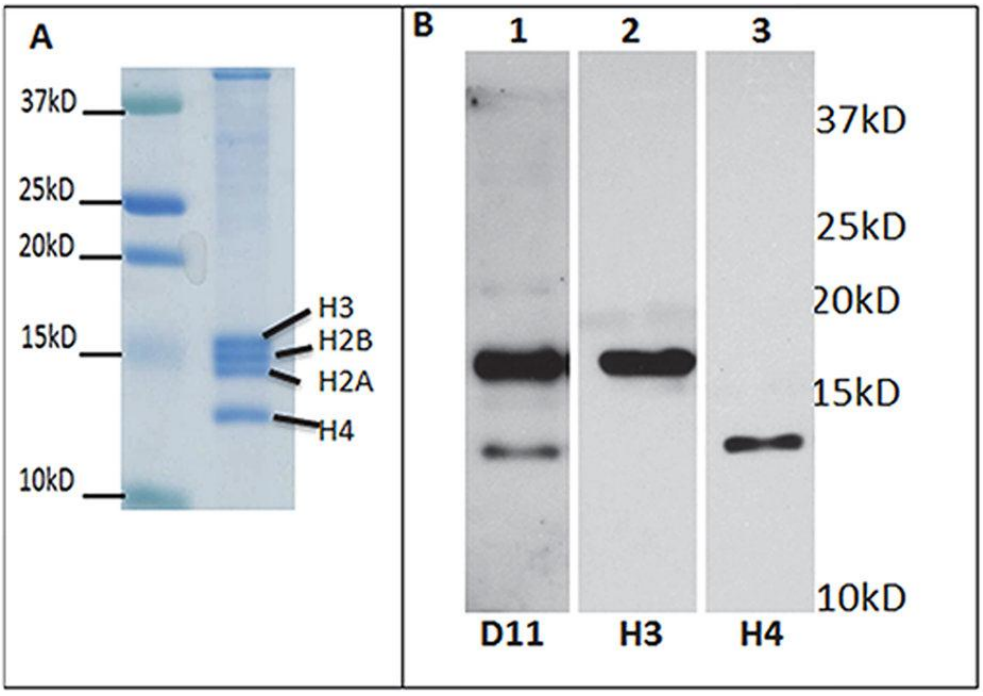

Figure 12: Confirmation of γKA-modified histone-H3 and histone-H4. (A) Coomassie staining of histones isolated from mouse lung; (B) Immunoblot of isolated histones using D11 ScFv (lane 1), Histone H3 (lane 2) or H4 (lane 3) antibody. (Mont S. et al, Sci Reports 2016)[97]

CHAPTER V

ACCUMULATION OF γKA-MODIFIED PROTEIN IS PRESENT IN OXIDATIVE STRESS MEDIATED PULMONARY INJURY

Results:

Ionizing radiation promotes the formation of γKA-modified proteins. Seventy percent of X- and gamma-ray photons traversing a tissue interact with water molecules that rapidly decompose into hydroxyl radicals (•OH), hydrogen radicals (•H), hydrogen peroxide, superoxide, and solvated electrons[102]. It was investigated if ionizing radiation could generate γKA-modified protein in a cell culture model. Although alveolar epithelial cells and fibroblasts are key to the pathogenesis of radiation–induced pulmonary fibrosis[103], their response may be a consequence to radiation-induced pulmonary microvascular injury, a prominent feature that manifests hours after irradiation of human, dog, rat, and mouse lung[104–109]. Based on this knowledge, endothelial cells were used to induce formation of γKA-modified proteins. Human Microvascular Endothelial Cells (HMVECs) were exposed to 5 Gy of Cesium-137 γ-rays. Quantification of immunofluorescence D11 staining for γKA-modified proteins show a 2-fold increase 24 hours after irradiation ($P = 0.001$, see figure 13). Because hydrogen peroxide (H_2O_2) is formed following photon irradiation, it was determined if H_2O_2 would induce γKA-modification. HMVECs were exposed to 150 μM H_2O_2 for 1hr at 37°C and then allowed to recover for 24 hrs prior to immunostaining with D11. Hydrogen peroxide treatment caused a 4.4 fold increase in γKA-modified protein ($P = 8.4 \times 10^{-7}$ see figure 13).

γKA-modified proteins are cytotoxic and promote apoptosis. To determine the consequence of increasing the cellular burden of γKA-modified protein, 3B11 and HMVECs were exposed to a bolus of a synthetic γKA isomer (15-E_2-IsoLG in PBS (1 μM/1 hr). 15-E_2-IsoLG is one of the γKA regioisomers that can be produced by both the free radical pathway and the cyclooxygenase pathway (i.e. levuglandin E2) and its synthesis was described in Lipids in Health and Disease[110]. Apoptosis induced by 15-E_2-IsoLG was then assessed 16 hrs later by quantifying Annexin V positive/propidium iodine negative staining (see figure 14). Exposure to 15-E_2-IsoLG (EC50 = 1 μM) produced statistically significant increases in apoptosis, as measured by Annexin V positive/propidium iodine negative staining in both cell types.

Alveolar epithelial type II cells are a key component to development of pulmonary fibrosis[103]. Therefore it was of interest to determine if type II cells were susceptible to γKA-mediated cytotoxicity. SV40 transformed mouse MLE12 alveolar type II cells were exposed to various concentrations of 15-E_2-IsoLG for 1 hr in PBS. Cytotoxicity, as measured by a MTT assay, was quantified 16 hrs later (see figure 14).

Accumulation of γKA-modified protein in irradiated lung tissue. Suppression of Nrf2 and elevation of NADPH oxidase-mediated oxidant stress as disease progresses[74,111,112] are two prominent features of radiation-induced pulmonary injury and human IPF[74,113–116]. It was thus investigated whether γKA protein modification also accompanies radiation injury. Wild type C57BL/6J mice were administered a thoracic dose of 16 Gy, a dose that induces fibrotic lesions within 16 weeks[106]. Strikingly, 16 Gy significantly increased the degree of D11-mediated immunofluorescence 6 and 16

weeks after irradiation. Six weeks after 16 Gy there was a nearly 3-fold increase, which increased a further 2.3 fold 16 weeks after treatment as compared to sham control (see figure 15). These findings correlate the onset and persistence of pulmonary fibrosis with the formation and accumulation of γKA-modified proteins.

γKA-modified proteins are present in human IPF tissue. Having shown that γKA-modified proteins are present in a murine model of pulmonary fibrosis it was of interest to determine if human IPF tissue would have a similar phenotype. Human lung tissue was obtained from 3 organ donor individuals and 3 IPF patients who underwent lung transplant. Fibrotic tissue present in IPF samples is apparent by H&E staining (see figure 16). Comparison of D11 immunofluorescence staining among the samples revealed a 4-fold increase in γKA-modified proteins in IPF tissue compared to organ donor controls ($P = 5.8x10^{-41}$, N = 100 fields, see figure 16). Inspection of IHC staining using the D11 antibody and counterstained with methyl green indicated the presence of γKA-modified protein in single cells and in multi-cellular lesions (see figure 17).

IPF dense fibrotic tissue was co-immunostained for collagen1α1 and γKA-modified protein. As illustrated in figure 18, γKA-modified protein co-localized with collagen1α1 in IPF tissue, consistent with the results obtained from the MS analysis ((see database table published by Mont S. et al, Scientific Reports, 2016: *Supplementary Table S2,* tab structural (GO: 0005198))[97].

γKA-modified collagen impairs MMP-1 mediated degradation. Having shown that γKA-modified proteins colocalize in with collagen1α1 in IPF tissue, it was hypothesizied that this modification may inhibit MMP mediated degradation. To test this hypothesis, collagen1α1 was modified with synthetic 15-E_2-IsoLG. Results from this assay demonstrated that 15-E_2-IsoLG modification of collagen1α1 impaired its degradation by MMP1 in a concentration-dependent manner (see figure 19). This finding is consistent with the results reported by Davies et al. who have shown that γKA modification of protein impedes its proteolysis[117].

Figure 13

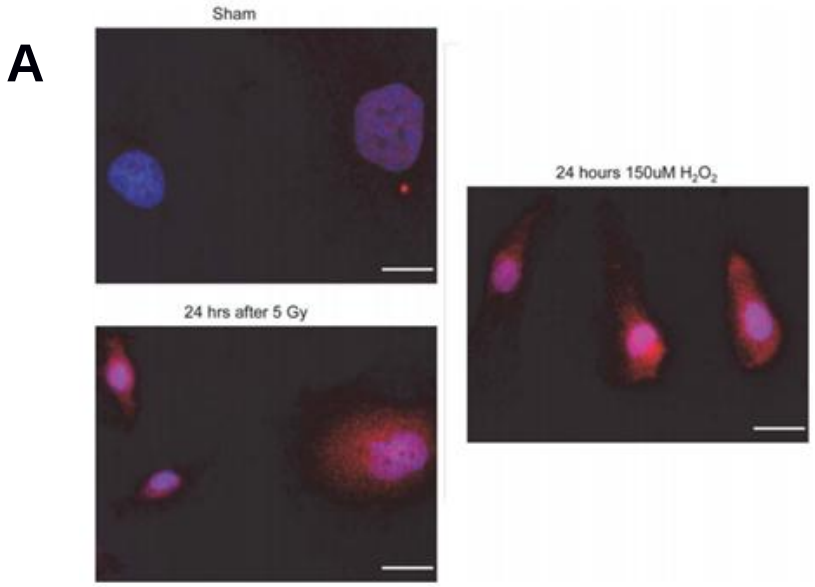

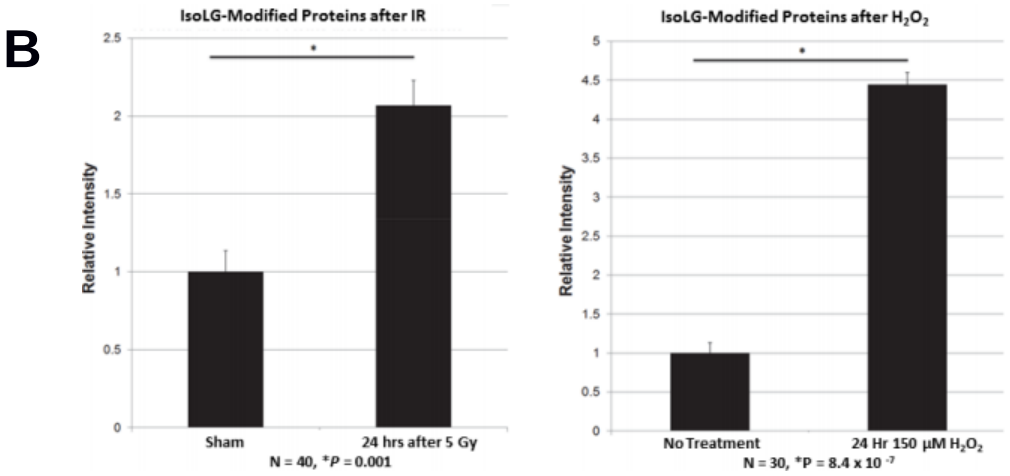

Figure 13: Ionizing radiation promotes the formation of γKA-modified proteins. A) Ionizing radiation and hydrogen peroxide induce formation of IsoLG-modified proteins. Human microvascular endothelial cells were stained for IsoLG-protein-adducts (Red) before and 24 hrs after administration of 5 Gy of γ-rays or 150uM hydrogen peroxide. B) Relative D11 staining intensity normalized to no treatment controls. Staining was measured at 60x magnification by wide-field microscopy and quantified by NIS Elements AR (Nikon). (Mont S. et al, Sci Reports 2016)[97]

Figure 14

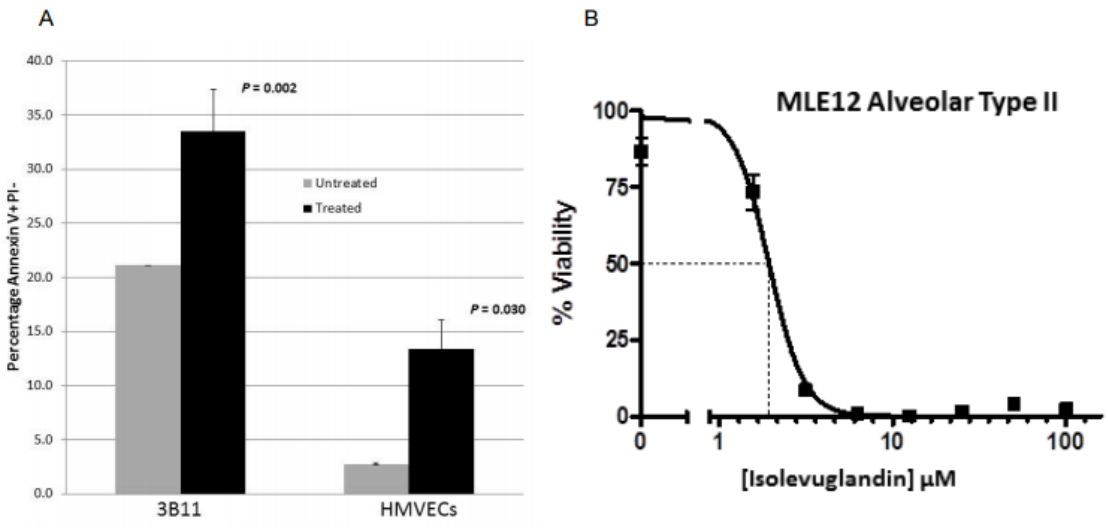

Figure 14: γKA-modified proteins are cytotoxic and promote apoptosis. A) Apoptosis of 3B11 and HMVECs exposed to 1µM 15-E2-IsoLG for 1 hr. Sixteen hrs later apoptosis was measured by Annexin V+ PI- stained cells (mean ±SD, N = 3). B) Loss of viability in MLE12 cells exposed to various concentrations of 15-E2-IsoLG for 1 hr. Sixteen hrs later an MTT assay was used to quantify viability (mean ±SD, N = 4). Standard deviations are shown if larger than symbols. (Mont S. et al, Sci Reports 2016)[97]

Figure 15

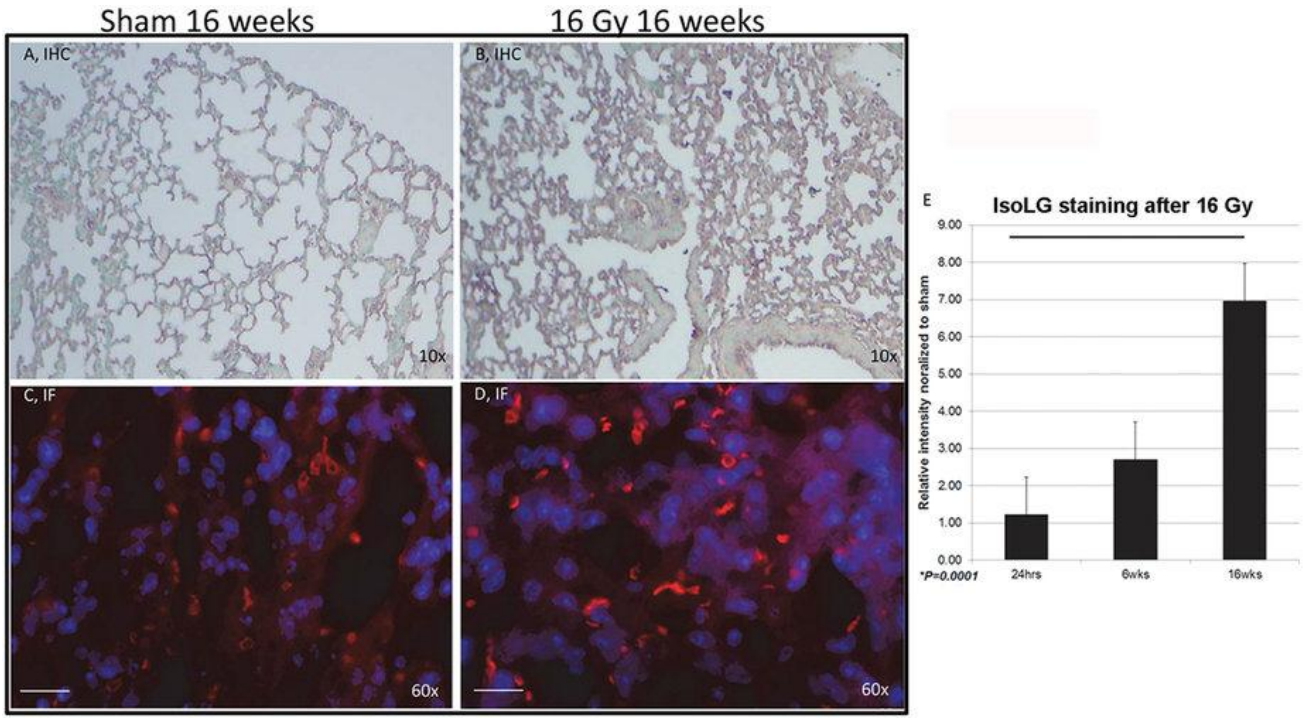

Figure 15: Accumulation of γKA-modified protein in irradiated lung tissue. Mouse pulmonary tissue was obtained 16 weeks after exposure to sham irradiation (A,C) or 16 Gy (B,D). (A,B) IHC D11 ScFv immunostaining, counterstained with methyl green. (C,D) D11 ScFv immunofluorescence (IF) counterstained with DAPI. Random fields are shown. (E) Mean (±SD) immunofluorescence staining was measured at 60× magnification by wide-field microscopy (40 fields per time point obtained from 12 mice). White bar represents 30 µm. (Mont S. et al, Sci Reports 2016)[97]

Figure 16

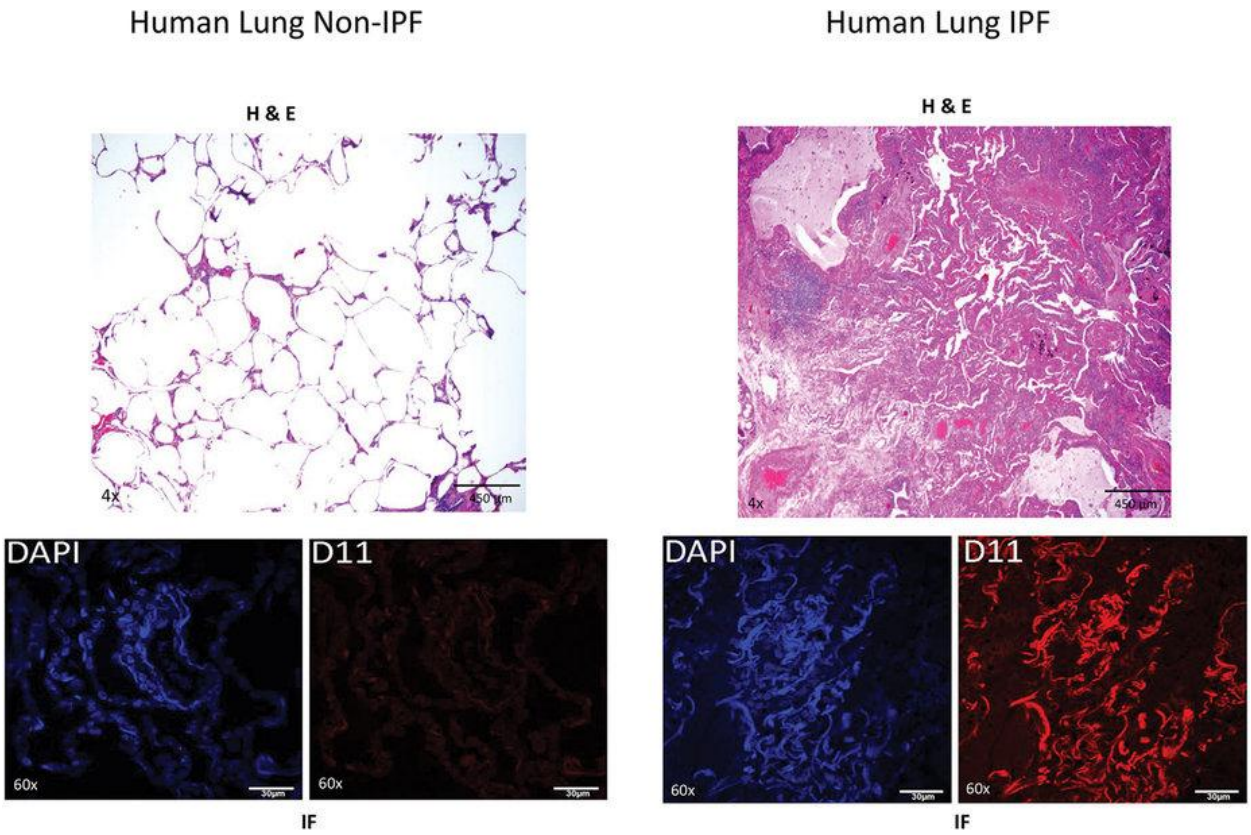

Figure 16: γKA-modified proteins are present in human IPF tissue. FFPE sections underwent H&E staining. Sections were imaged using wide field microscopy. Other sections were imaged by confocal microscopy following immunofluorescent staining with D11 ScFv and counter staining with DAPI. White bars in IF sections represent 30 µm. (Mont S. et al, Sci Reports 2016)[97]

Figure 17

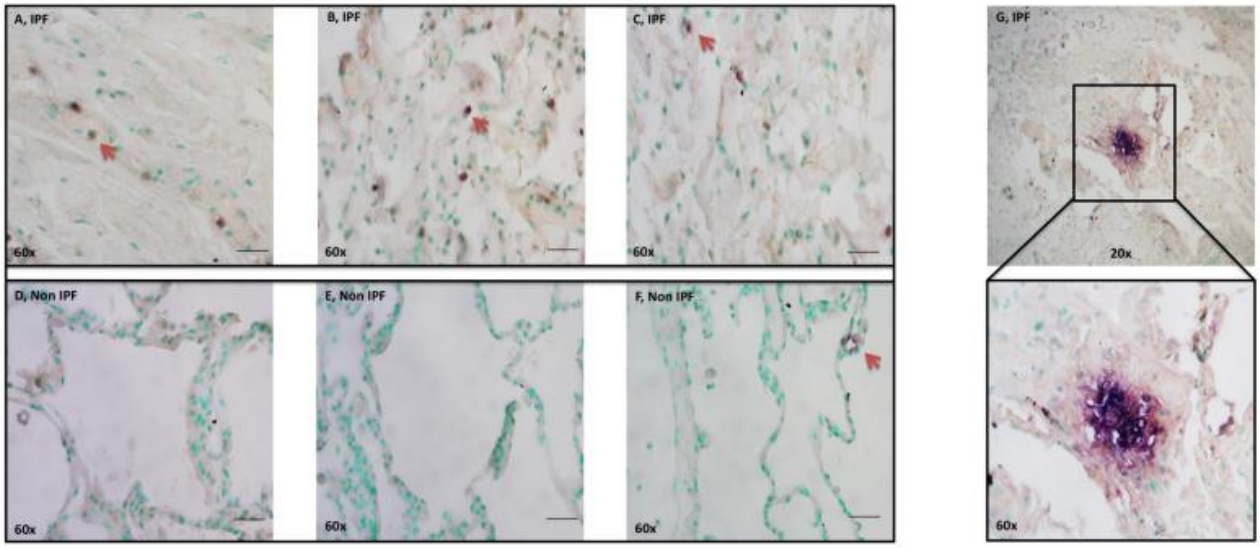

Figure 17: γKA-modified protein in single cells and in multi-cellular lesions in IPF vs non IPF tissue. Human lung tissue sections obtained from IPF patients (panels A-C & G) or non-IPF organ donors (panels D-F). FFPE sections were subjected to IHC staining with D11 and counter stained with methyl green. Sections were imaged using wide field microscopy. Black bar represents 30 μM. Red arrowhead denotes positively stained cells in panels A- F. (Mont S. et al, Sci Reports 2016)[97]

Figure 18

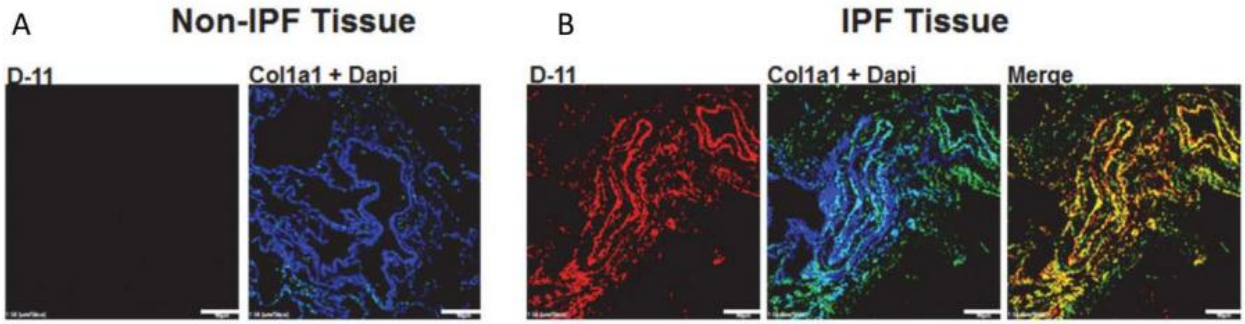

Figure 18: γKA-modified proteins are present in human idiopathic pulmonary fibrotic tissue and colocalize with collagen. Human lung tissue sections from an organ donor (A) or from a subject with IPF (B) were stained with D11 (Red) and collagen type 1 alpha 1 (Alexa 647, green false color) and imaged by confocal microscopy. 20x magnification, N= 150 fields. The white bar represents 30 μm. (Mont S. et al, Sci Reports 2016)[97]

Figure 19

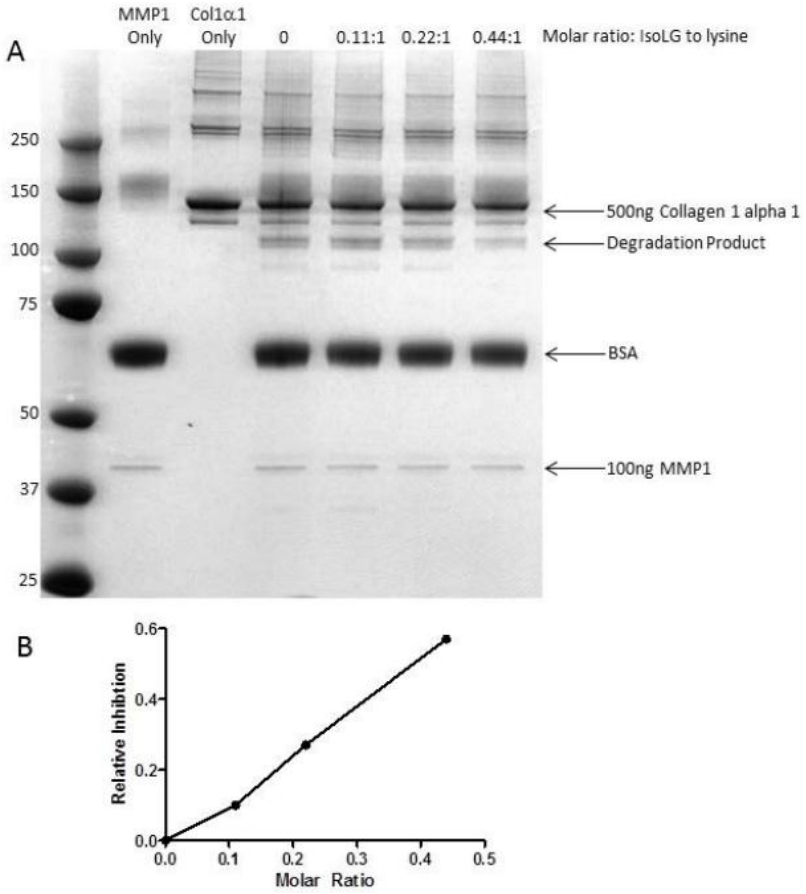

Figure 19: γKA-modified collagen impairs MMP-1 mediated degradation. A) Purified human recombinant Col1α1 was incubated with the indicated molar ratios of purified IsoLG at 37°C/1hr, after which unreacted IsoLG was quenched. MMP1 was the added to the reaction and incubated at 37°C/0.5hr, pH = 7.0. Col1α1 degradation was analyzed by 1D SDS PAGE, Coomassie Blue staining. B) Intensity of Col1α1 degradation product was quantified and is shown as relative inhibition. (Mont S. et al, Sci Reports 2016)[97]

CHAPTER VI

SUMMARY AND DISCUSSION

Although it is well established that oxidative stress promotes progression of many diseases, the underlying mechanisms are not well understood. As shown by emerging research, γKAs are a proteotoxic and immunogenic stress that links ROS to progression of disease[2,94,95,118,119]. The work of this dissertation, suggests that γKA-modified protein has a significant presence in radiation-induced pulmonary injury and IPF (see figure 20). In addition, genetic regulators of oxidative stress play a critical role in the formation and accumulation of γKA-modified protein (see figure 21). Furthermore, data demonstrating that γKA is proapoptotic and modifies collagen in IPF tissue and that modified collagen is resistant to proteolysis by MMP1 point to γKA as one plausible mechanism driving chronic pulmonary injury and fibrosis (see figure 22).

As a significant amount of the data was developed using a single chain antibody, termed D11[92], that specifically recognizes IsoLG-lysyl adducts in protein, the specificity of the antibody requires addressing. Immunoreactivity is independent of peptide sequence and adjacent polar or acidic residues. Competition assays against the D11 epitope show that it specifically binds to adducts from oxidized arachidonyl-lysine but not by non-oxidized arachidonyl-lysine[92]. Furthermore, D11 does not cross react with hydroxynonenal (HNE) or oxononanal (ONA) adducted RKDVY peptide. The nonreactive F2-isoprostane product, 15-F2t-IsoP (8-isoPGF2a), also does not compete for D11[92]. Finally, we demonstrated that blocking the D11 epitope using IsoLG reacted with excess free lysine abrogates immunoreactivity with mouse lung tissue (unpublished

data and [92]). The strength of using the D11 antibody is that it can recognize the IsoLG-lysyl adducts independent of protein identity. This allows for a broad inspection of γKA-modified proteins and the ability to immunoprecipitate several different protein targets for mass spectrometry analysis. However one limitation of using D11 is that during immunoprecipitation the antibody may only immunopurify proteins with several IsoLG-lysyl adducts and potentially miss proteins which are not as heavily modified. Additionally, a target specific antibody would need to be generated to identify IsoLG-lysyl adducts on specific protein targets. This limitation currently only allows to immunoprecipitate or purify target proteins and then assess IsoLG-lysyl adduct by immunoblot studies.

The presence of γKA-modified protein in alveolar epithelium and endothelium, as well as in bronchiolar epithelium of healthy mice indicates that cells can tolerate a basal level of protein modification. This demonstrates that a cell's γKA load is directly related to its oxidant burden. Nox2 catalyzes electron transfer from NADPH to molecular oxygen, generating superoxide, which can dismutate into H_2O_2[98] and is expressed in most pulmonary cells, including alveolar macrophages, and dendritic cells[120]. The importance of Nox2 as a major cellular source of oxidant stress driving γKA modification in the lung is underscored by the reduction in D11 immunostaining in $p47^{phox}$ deficient mice. Although the free radical pathway is a likely route of γKA formation under these conditions, the cyclooxygenase pathway of γKA formation may also contribute as formation of ROS by Nox can upregulate COX2 activity[121,122]. Nrf2, which is ubiquitously expressed, promotes antioxidant gene expression (eg, SOD1, SOD2, and CAT) and is critical for maintaining ROS homeostasis[18]. The results from this dissertation

demonstrates that pulmonary tissue from Nrf2-null mice exhibited significantly increased levels of γKA-modified protein, thus identifying Nrf2 gene expression as important for the suppression of modification.

Immuno-isolation of γKA-modified protein followed by MS/MS analysis identified over 160 protein targets. Although irradiation produced significantly more modification, the majority of the proteins were the same for irradiated and non-irradiated cells. One interpretation for these results is that cells contain a pool of susceptible protein, so that increasing the oxidant stress primarily increases the fraction of each susceptible protein within the pool that is modified. PANTHER network analysis revealed that proteins from multiple organelles and pathways are susceptible to be modified.

Proteins modified by γKAs can be a proteotoxic event, a consequence of protein misfolding, aggregation, and/or crosslinking[101,123–127]. Davies et al. have shown that γKA-modified proteins are poor substrates for proteasome-dependent degradation and that the proteasome itself can also be significantly impaired by γKA-modification[117]. One interpretation of the presented results is that γKA-mediated cytotoxicity is not a consequence of targeting a specific prosurvival pathway, but is most likely due to the accumulation of toxic modified proteins that exceed a critical threshold. Given that this modification is not specific to a class of organelles or cellular pathways, determining the exact concentration of all susceptible proteins to this modification would be challenging. However, to attempt to answer this question one may focus on a particular set of proteins which may be involved in the clearance of adducted proteins or involved in redox homeostasis, as their inability to function would have a direct effect to increasing the concentration of γKA-modified proteins.

Ionizing radiation is a well characterized prooxidant and was shown to induce γKA protein-modification in cell culture and in a murine model of radiation-induced pulmonary fibrosis. It is well established that most chronic fibrotic diseases have in common a state of persistent injury[128]. Thus it was of particular interest to observe that ionizing radiation produces a state of chronic γKA protein-modification that correlates with chronic apoptosis and fibrosis[86]. γKA-modified proteins were also found to be a prominent feature of IPF. Collagen1α1 was shown to be modified by γKAs in IPF patients. This modification was also demonstrated to impair MMP1 mediated degradation, demonstrating the potential to induce a state of chronic injury and to impair resolution of established fibrosis. In summary, these results suggest that the excess oxidant burden associated with radiation-induced pulmonary fibrosis and with IPF drives the hitherto unrecognized pathogenic accumulation of γKA-modified protein. Since γKA can be proteotoxic and injurious to cells, γKA may not only be a marker of oxidant-stressed cells, but also augments lung injury and fibrosis.

Figure 20

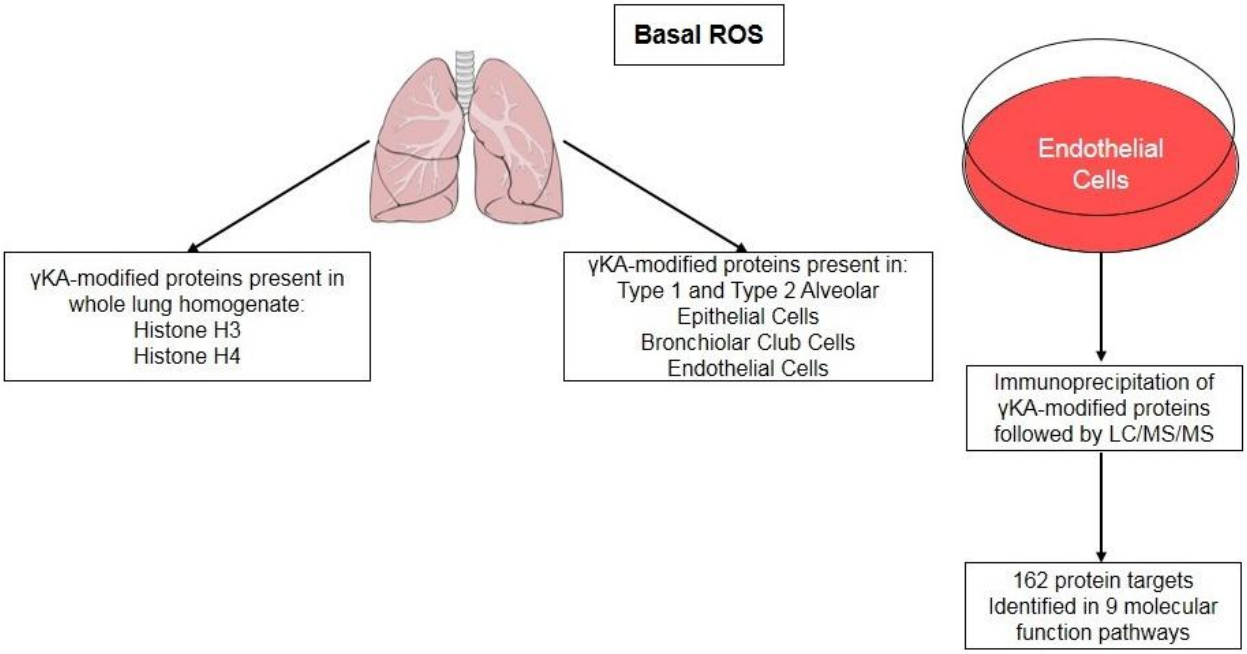

Figure 20: Generation of γKA-modified proteins under basal conditions.

Figure 21

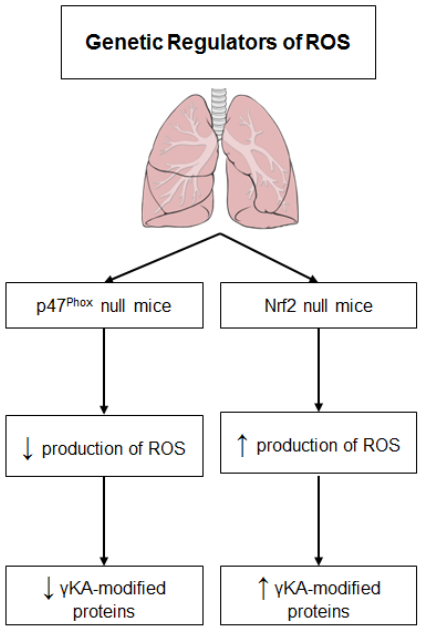

Figure 21: Genetic regulators of γKA production in lung tissue.

Figure 22

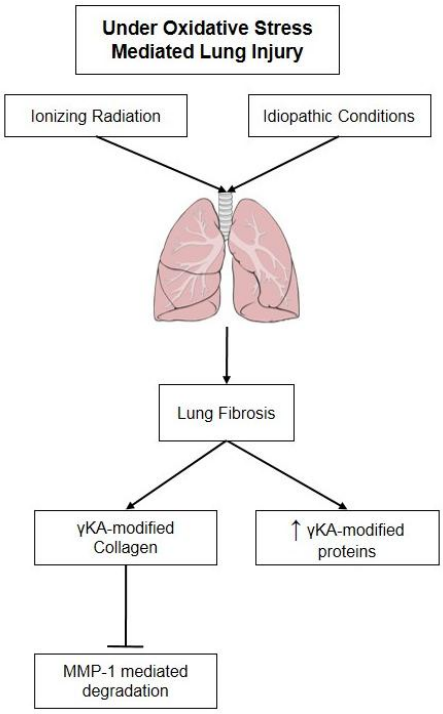

Figure 22: γKA production under oxidative stress mediated lung injury.

CHAPTER VII

SIGNIFICANCE AND FUTURE DIRECTIONS

Understanding the consequence of oxidative stress mediated lung injury has broad implications and impact in the treatment of pulmonary fibrosis. Treatment for pulmonary fibrosis is crucial for patients undergoing radiation therapy or patients undergoing chemotherapy where late onset of lung fibrosis leading to increased mortality is a known potential side-effect[129]. In these cases finding a treatment that can be used to prevent the development of fibrosis during and after therapy would be greatly beneficial. For patients with idiopathic pulmonary fibrosis finding a treatment to treat established fibrosis is also crucial. Currently, the drug Salicylamine has been shown to react with free γKA molecules thus blocking the ability of γKA to bind to protein[130,131]. This drug has been demonstrated to be effective in mouse models of oxidative stress mediated diseases such hypertension[94] and Alzheimer's disease[132]. To determine if this drug can help prevent the onset of pulmonary fibrosis, Salicylamine can be administered before and during lung injury using mouse models of radiation-induced fibrosis and chemotherapy induced fibrosis (eg, Bleomycin). Salicylamine can also be given after established fibrosis in mouse models and survival studies can help determine if treatment can stop the progression of fibrosis and extend survival.

Understanding the consequence of γKA-modified proteins has broad implications and impact in the context of cellular biology. It is currently not well understood how cells can maintain a basal level of γKA-modified proteins. To this end, understanding how γKA-modified proteins can affect protein degradation and protein turnover is crucial.

Eukaryotes use two major pathways to clear proteotoxic proteins: ubiquitination/proteasome-mediated degradation[133] and autophagy[134]. Davies et al. have shown that γKA-modified proteins are poor substrates for proteasome-dependent degradation and that the proteasome itself can also be significantly impaired by γKA-modification[117]. However, the direct mode of action of how γKA protein-modification impairs proteosomal mediated degradation remains to be determined. To elucidate what occurs upon γKA adduction, one approach would be to use a his-tagged target protein which is modified by γKA in-vitro and then introduced into cells which are transfected with cDNA-plasmid expressing HA-tagged polyubiquitin. The his-tagged target protein can be introduced into a mammalian cell using dfTAT[135], which is an endosomolytic agent that can deliver whole protein molecules into cells without toxicity, at a concentration where the adducted protein does not induce cell death. His-tagged target protein modified by γKA can then be purified from cells using nickel resin columns. Immunoblotting his-tagged proteins against the HA tag will then determine if this γKA-modified protein is modified by polyubiquitin and targeted for proteosomal degradation (see figure 23). To confirm the results of this study degradation of the his-tagged target protein can be measured using a cell culture model containing a temperature sensitive mutation for the ubiquitin-activating enzyme E1. This mouse cell line, ts20 expresses wild-type functional E1 at 35°C but at 39°C the E1 enzyme activity is inhibited resulting in the accumulation of ubiquitinated substrates[136]. Immunoblotting his-tagged proteins following purification using a nickel resin column at each temperature can determine if the target protein can be targeted for degradation by the E1 enzyme (see figure 24).

Currently, it has not been investigated whether the autophagy pathway is impacted by γKA protein-modification. One method to help elucidate the role of γKA-modified proteins in autophagy, is to modify green-fluorescently tagged target protein modified in-vitro with γKA (at various molar-ratio concentrations). The target protein can be introduced into a mammalian cell culture system using dfTAT[135]. Upon introducing the γKA modified target protein in cells, live cellular imaging along with LysoProbe-dye which labels lysosomes in red-fluorescence[137], can be used to track the degradation of γKA-modified proteins. Colocalization of green-fluorescence and red-fluorescence can be used to measure and locate the degradation of γKA-modified proteins. In order to ensure that the degradation is lysosome dependent, cells can be pretreated with a proteosomal inhibitor MG132[138] (see figure 25).

Understanding and identifying the specific lysine residues which are modified by γKAs has broad implications and impact in the context of biochemistry and protein function. In this study histones H3 and H4 were found to be modified by γKA when isolated in whole lung homogenates. Histones are key proteins involved in the capacity for DNA to be accessible or not accessible to genetic regulation. They are therefore directly involved in epigenetic changes and involved in cellular development and differentiation[139]. Histone acetylation and methylation occur on lysine residues and thus investigating if γKA can bind to these lysine residues is important. One method to determine what lysine residues can be modified is outlined by Charvet, C. D. and Pikuleva, I. A.[140]. The key approach of this method relies in creating a mass spectrometry profile from adducting purified protein in-vitro and then subjecting the modified protein to LC/MS/MS. Once a mass-shift profile is identified, it can be used to

identify modified proteins in-vivo. The specific lysine residue can then be confirmed by adducting a protein with a mutational change in a specific lysine residue into another positively charged amino acid (eg, histidine, asparagine). To determine how γKA modification affect histone modifications, a histone modification assay, developed by Epigentek can be used on adducted histones. In this assay, 21 different histone modifications can be measured and quantified, corresponding to specific methylation or acetylation states on specific lysine residues[141–145].

In summary this dissertation identifying γKA-modified protein as a feature of basal ROS production in lung tissue and its accumulation in oxidative stress mediated lung injury allows for future studies to develop new therapeutics for pulmonary fibrosis as well as allow for an additional understanding of γKA-modification within the context of cellular biology.

Figure 23

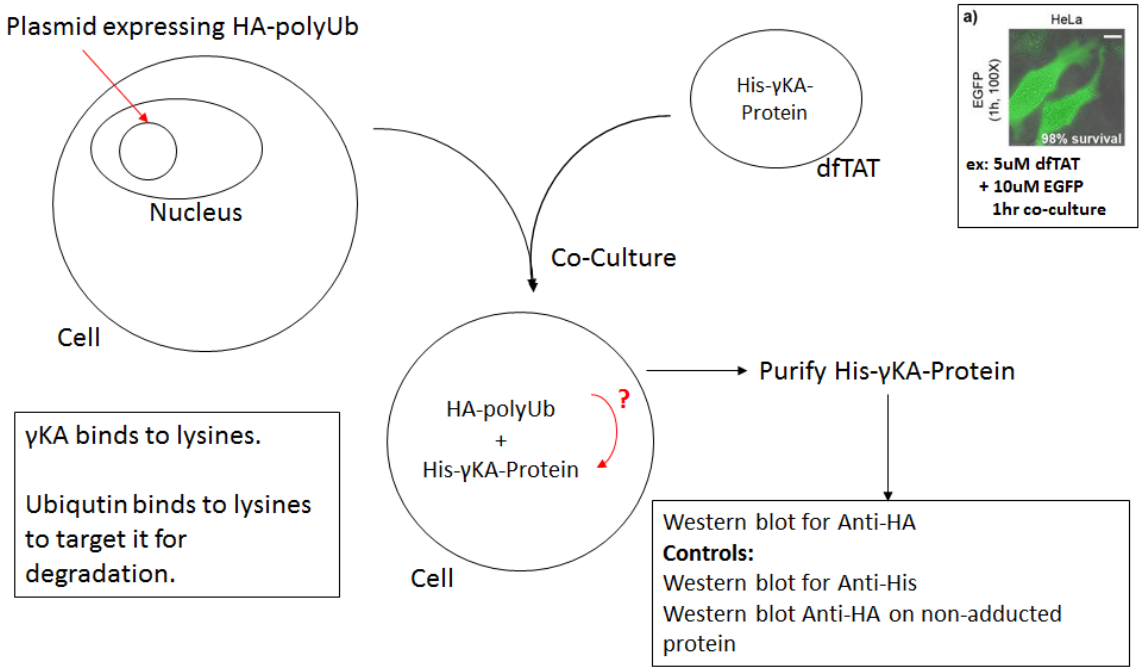

Figure 23: Summary of experimental design to determine if γKA-modification impairs ubiquitin binding to target protein.

Figure 24

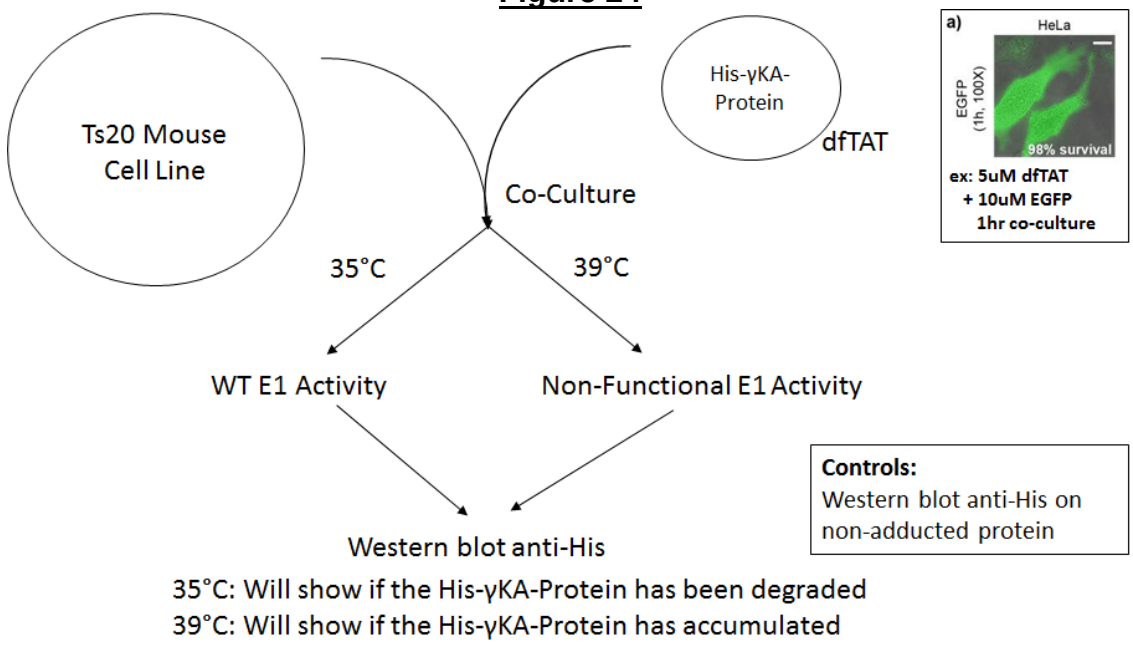

Figure 24: Summary of experimental design to determine if γKA-modification impairs ubiquitin-activating enzyme E1 activity.

Figure 25

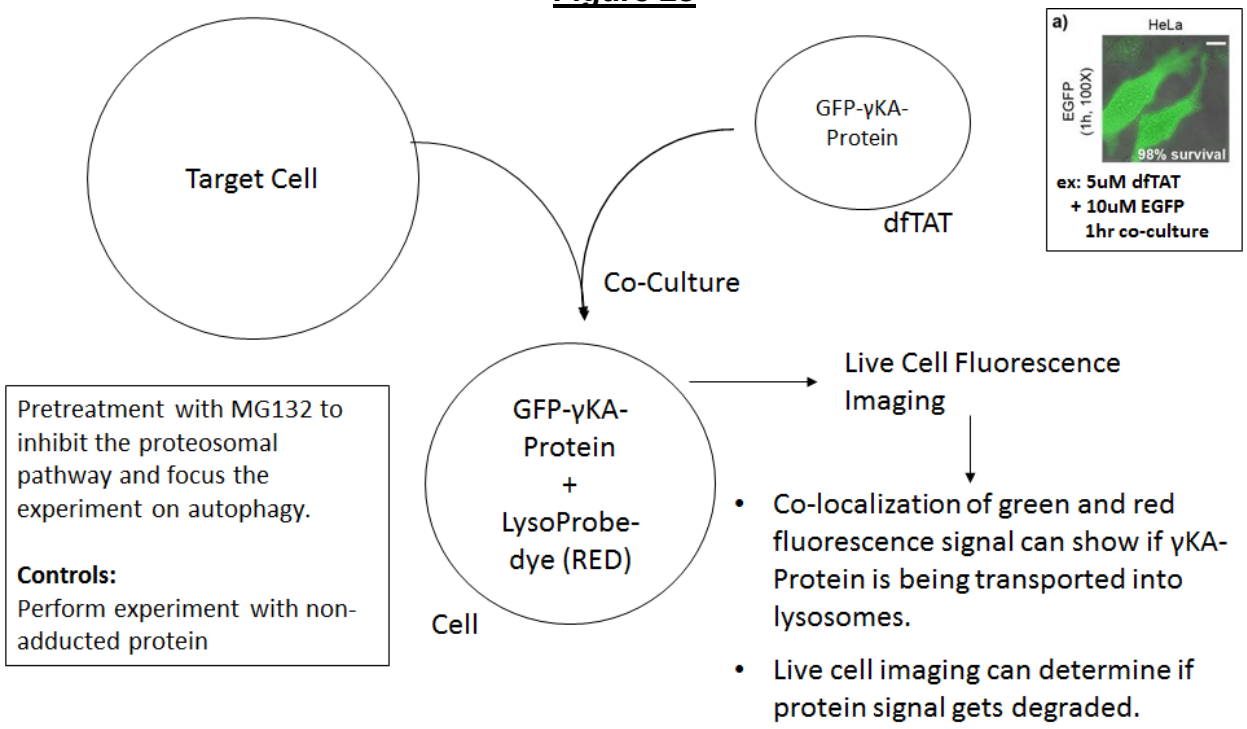

Figure 25: Summary of experimental design to determine if γKA-modification impairs lysosome-mediated protein degradation.

REFERENCES

1. Pace-Asciak, C. R. Oxidative biotransformations of arachidonic acid. *Prostaglandins* **13,** 811–817 (1977).

2. Davies, S. S. *et al.* Supplement Data - Treatment with a γ-ketoaldehyde scavenger prevents working memory deficits in hApoE4 mice. *J. Alzheimers. Dis.* **27,** 49–59 (2011).

3. Montuschi, P., Barnes, P. J. & Roberts, L. J. 2nd. Isoprostanes: markers and mediators of oxidative stress. *FASEB J. Off. Publ. Fed. Am. Soc. Exp. Biol.* **18,** 1791–1800 (2004).

4. Davies, S. S., Amarnath, V. & Roberts, L. J. Isoketals: highly reactive γ-ketoaldehydes formed from the H2-isoprostane pathway. *Chem. Phys. Lipids* **128,** 85–99 (2004).

5. Salomon, R. G., Jirousek, M. R., Ghosh, S. & Sharma, R. B. Prostaglandin endoperoxides 21. Covalent binding of levuglandin E2 with proteins. *Prostaglandins* **34,** 643–56 (1987).

6. Brame, C. J., Salomon, R. G., Morrow, J. D. & Roberts, L. J. Identification of extremely reactive gamma-ketoaldehydes (isolevuglandins) as products of the isoprostane pathway and characterization of their lysyl protein adducts. *J. Biol. Chem.* **274,** 13139–13146 (1999).

7. Auten, R. L. & Davis, J. M. Oxygen toxicity and reactive oxygen species: the devil is in the details. *Pediatr. Res.* **66,** 121–7 (2009).

8. Wang, K. *et al.* Redox homeostasis: the linchpin in stem cell self-renewal and differentiation. *Cell Death Dis.* **4,** e537 (2013).

9. Bernard, K., Hecker, L., Luckhardt, T. R., Cheng, G. & Thannickal, V. J. NADPH oxidases in lung health and disease. *Antioxid. Redox Signal.* **20,** 2838–53 (2014).

10. Kleniewska, P., Piechota, A., Skibska, B. & Gorăca, A. The NADPH oxidase family and its inhibitors. *Arch. Immunol. Ther. Exp. (Warsz).* **60,** 277–294 (2012).

11. Vignais, P. V. The superoxide-generating NADPH oxidase: structural aspects and activation mechanism. *Cell. Mol. Life Sci.* **59,** 1428–59 (2002).

12. Lambeth, J. D. & Neish, A. S. Nox enzymes and new thinking on reactive oxygen: a double-edged sword revisited. *Annu. Rev. Pathol.* **9,** 119–45 (2014).

13. Zhang, D. D., Lo, S.-C., Cross, J. V, Templeton, D. J. & Hannink, M. Keap1 is a redox-regulated substrate adaptor protein for a Cul3-dependent ubiquitin ligase complex. *Mol. Cell. Biol.* **24,** 10941–53 (2004).

14. Kobayashi, A. *et al.* Oxidative stress sensor Keap1 functions as an adaptor for Cul3-based E3 ligase to regulate proteasomal degradation of Nrf2. *Mol. Cell. Biol.* **24,** 7130–9 (2004).

15. Zhang, D. D. & Hannink, M. Distinct cysteine residues in Keap1 are required for Keap1-dependent ubiquitination of Nrf2 and for stabilization of Nrf2 by chemopreventive agents and oxidative stress. *Mol. Cell. Biol.* **23,** 8137–51 (2003).

16. Baird, L., Llères, D., Swift, S. & Dinkova-Kostova, A. T. Regulatory flexibility in the Nrf2-mediated stress response is conferred by conformational cycling of the Keap1-Nrf2 protein complex. *Proc. Natl. Acad. Sci. U. S. A.* **110,** 15259–64 (2013).

17. Wasserman, W. W. & Fahl, W. E. Functional antioxidant responsive elements. *Proc. Natl. Acad. Sci. U. S. A.* **94,** 5361–6 (1997).

18. Nguyen, T., Nioi, P. & Pickett, C. B. The Nrf2-antioxidant response element signaling pathway and its activation by oxidative stress. *J. Biol. Chem.* **284,** 13291–5 (2009).

19. Kobayashi, M. & Yamamoto, M. Molecular mechanisms activating the Nrf2-Keap1 pathway of antioxidant gene regulation. *Antioxid. Redox Signal.* **7,** 385–94 (2005).

20. Chen, J., Zhang, Z. & Cai, L. Diabetic cardiomyopathy and its prevention by nrf2: current status. *Diabetes Metab. J.* **38,** 337–45 (2014).

21. Downs, C. a *et al.* β-Adrenergic agonists differentially regulate highly selective and nonselective epithelial sodium channels to promote alveolar fluid clearance in vivo. *Am. J. Physiol. Lung Cell. Mol. Physiol.* **302,** L1167–78 (2012).

22. Goodson, P. *et al.* Nadph oxidase regulates alveolar epithelial sodium channel activity and lung fluid balance in vivo via O^{-}_{2} signaling. *Am. J. Physiol. Lung Cell. Mol. Physiol.* **302,** L410–9 (2012).

23. Fu, P. *et al.* Role of nicotinamide adenine dinucleotide phosphate-reduced oxidase proteins in Pseudomonas aeruginosa-induced lung inflammation and

permeability. *Am. J. Respir. Cell Mol. Biol.* **48,** 477–88 (2013).

24. Peshavariya, H. M., Chan, E. C., Liu, G. S., Jiang, F. & Dusting, G. J. Transforming growth factor-β1 requires NADPH oxidase 4 for angiogenesis in vitro and in vivo. *J. Cell. Mol. Med.* **18,** 1172–83 (2014).

25. Sutcliffe, A. *et al.* Increased nicotinamide adenine dinucleotide phosphate oxidase 4 expression mediates intrinsic airway smooth muscle hypercontractility in asthma. *Am. J. Respir. Crit. Care Med.* **185,** 267–74 (2012).

26. Ceriello, A. Possible role of oxidative stress in the pathogenesis of hypertension. *Diabetes Care* **31 Suppl 2,** S181–4 (2008).

27. Chatterjee, M., Saluja, R., Kanneganti, S., Chinta, S. & Dikshit, M. Biochemical and molecular evaluation of neutrophil NOS in spontaneously hypertensive rats. *Cell. Mol. Biol. (Noisy-le-grand).* **53,** 84–93 (2007).

28. Dröge, W. Free radicals in the physiological control of cell function. *Physiol. Rev.* **82,** 47–95 (2002).

29. Basu, S., Whiteman, M., Mattey, D. L. & Halliwell, B. Raised levels of F(2)-isoprostanes and prostaglandin F(2alpha) in different rheumatic diseases. *Ann. Rheum. Dis.* **60,** 627–31 (2001).

30. Valko, M. *et al.* Free radicals and antioxidants in normal physiological functions and human disease. *Int. J. Biochem. Cell Biol.* **39,** 44–84 (2007).

31. Walston, J. *et al.* Serum antioxidants, inflammation, and total mortality in older women. *Am. J. Epidemiol.* **163,** 18–26 (2006).

32. Bhat, A. H. *et al.* Oxidative stress, mitochondrial dysfunction and neurodegenerative diseases; a mechanistic insight. *Biomed. Pharmacother. = Biomédecine pharmacothérapie* **74,** 101–10 (2015).

33. Götz, M. E., Freyberger, A. & Riederer, P. Oxidative stress: a role in the pathogenesis of Parkinson's disease. *J. Neural Transm. Suppl.* **29,** 241–9 (1990).

34. Bozzo, F., Mirra, A. & Carrì, M. T. Oxidative stress and mitochondrial damage in the pathogenesis of ALS: New perspectives. *Neurosci. Lett.* (2016). doi:10.1016/j.neulet.2016.04.065

35. Gałecki, P., Talarowska, M., Anderson, G., Berk, M. & Maes, M. Mechanisms underlying neurocognitive dysfunctions in recurrent major depression. *Med. Sci.*

Monit. **21,** 1535–47 (2015).

36. Hasselwander, O. & Young, I. S. Oxidative stress in chronic renal failure. *Free Radic. Res.* **29,** 1–11 (1998).

37. Wójcicka, G. & Bełtowski, J. [Oxidative stress in glomerulonephritis]. *Postępy Hig. i Med. doświadczalnej* **55,** 855–69 (2001).

38. Ziyadeh, F. N. & Wolf, G. Pathogenesis of the podocytopathy and proteinuria in diabetic glomerulopathy. *Curr. Diabetes Rev.* **4,** 39–45 (2008).

39. Williams, D. L. Oxidative stress and the eye. *Vet. Clin. North Am. Small Anim. Pract.* **38,** 179–92, vii (2008).

40. Berthoud, V. M. & Beyer, E. C. Oxidative stress, lens gap junctions, and cataracts. *Antioxid. Redox Signal.* **11,** 339–53 (2009).

41. Lou, M. F. Redox regulation in the lens. *Prog. Retin. Eye Res.* **22,** 657–82 (2003).

42. Montuschi, P. *et al.* 8-Isoprostane as a biomarker of oxidative stress in interstitial lung diseases. *Am. J. Respir. Crit. Care Med.* **158,** 1524–7 (1998).

43. Rahman, I. *et al.* Systemic and pulmonary oxidative stress in idiopathic pulmonary fibrosis. *Free Radic. Biol. Med.* **27,** 60–8 (1999).

44. Bargagli, E. *et al.* Oxidative stress in the pathogenesis of diffuse lung diseases: a review. *Respir. Med.* **103,** 1245–56 (2009).

45. Rahman, I. & MacNee, W. Oxidative stress and regulation of glutathione in lung inflammation. *Eur. Respir. J.* **16,** 534–54 (2000).

46. Mastruzzo, C., Crimi, N. & Vancheri, C. Role of oxidative stress in pulmonary fibrosis. *Monaldi Arch. chest Dis. = Arch. Monaldi per le Mal. del torace / Fond. Clin. del Lav. IRCCS [and] Ist. di Clin. Tisiol. e Mal. Appar. Respir. Univ. di Napoli, Second. ateneo* **57,** 173–6

47. Orr, C. R. & Jacobs, W. F. Pulmonary Fibrosis. *Radiology* **7,** 318–325 (1926).

48. Takishima, T. & Shimura, S. in *Basic and Clinical Aspects of Pulmonary Fibrosis* 293–304 (crcpress, 1994).

49. Hamman, L. & Rich, A. R. Fulminating Diffuse Interstitial Fibrosis of the Lungs.

Trans. Am. Clin. Climatol. Assoc. **51,** 154–63 (1935).

50. Harmman, L. Acute diffuse interstitial fibrosis of the lungs. *Bull. Johns Hopkins Hosp* **74,** 177 (1944).

51. Hopkins, R. B., Burke, N., Fell, C., Dion, G. & Kolb, M. Epidemiology and survival of idiopathic pulmonary fibrosis from national data in Canada. *Eur. Respir. J.* (2016). doi:10.1183/13993003.01504-2015

52. Schwartz, D. A. *et al.* Determinants of progression in idiopathic pulmonary fibrosis. *Am. J. Respir. Crit. Care Med.* **149,** 444–9 (1994).

53. Walters, D. M., Cho, H.-Y. & Kleeberger, S. R. Oxidative stress and antioxidants in the pathogenesis of pulmonary fibrosis: a potential role for Nrf2. *Antioxid. Redox Signal.* **10,** 321–32 (2008).

54. Panos, R. J., Mortenson, R. L., Niccoli, S. A. & King, T. E. Clinical deterioration in patients with idiopathic pulmonary fibrosis: causes and assessment. *Am. J. Med.* **88,** 396–404 (1990).

55. Raghu, G. *et al.* An official ATS/ERS/JRS/ALAT statement: idiopathic pulmonary fibrosis: evidence-based guidelines for diagnosis and management. *Am. J. Respir. Crit. Care Med.* **183,** 788–824 (2011).

56. Cross, C. E., van der Vliet, A., O'Neill, C. A., Louie, S. & Halliwell, B. Oxidants, antioxidants, and respiratory tract lining fluids. *Environ. Health Perspect.* **102 Suppl ,** 185–91 (1994).

57. American Thoracic Society. Idiopathic pulmonary fibrosis: diagnosis and treatment. International consensus statement. American Thoracic Society (ATS), and the European Respiratory Society (ERS). *Am. J. Respir. Crit. Care Med.* **161,** 646–64 (2000).

58. Kinder, B. W. *et al.* Baseline BAL neutrophilia predicts early mortality in idiopathic pulmonary fibrosis. *Chest* **133,** 226–32 (2008).

59. Rudd, R. M., Haslam, P. L. & Turner-Warwick, M. Cryptogenic fibrosing alveolitis. Relationships of pulmonary physiology and bronchoalveolar lavage to response to treatment and prognosis. *Am. Rev. Respir. Dis.* **124,** 1–8 (1981).

60. Boomars, K. A., Wagenaar, S. S., Mulder, P. G., van Velzen-Blad, H. & van den Bosch, J. M. Relationship between cells obtained by bronchoalveolar lavage and survival in idiopathic pulmonary fibrosis. *Thorax* **50,** 1087–92 (1995).

61. Kliment, C. R. & Oury, T. D. Oxidative stress, extracellular matrix targets, and idiopathic pulmonary fibrosis. *Free Radic. Biol. Med.* **49,** 707–17 (2010).

62. Manoury, B. *et al.* The absence of reactive oxygen species production protects mice against bleomycin-induced pulmonary fibrosis. *Respir. Res.* **6,** 11 (2005).

63. Selman, M. *et al.* Idiopathic pulmonary fibrosis: prevailing and evolving hypotheses about its pathogenesis and implications for therapy. *Ann. Intern. Med.* **134,** 136–51 (2001).

64. Collard, H. R. *et al.* Combined corticosteroid and cyclophosphamide therapy does not alter survival in idiopathic pulmonary fibrosis. *Chest* **125,** 2169–74 (2004).

65. Douglas, W. W. *et al.* Colchicine versus prednisone in the treatment of idiopathic pulmonary fibrosis. A randomized prospective study. Members of the Lung Study Group. *Am. J. Respir. Crit. Care Med.* **158,** 220–5 (1998).

66. Flaherty, K. R. *et al.* Steroids in idiopathic pulmonary fibrosis: a prospective assessment of adverse reactions, response to therapy, and survival. *Am. J. Med.* **110,** 278–82 (2001).

67. Thannickal, V. J., Toews, G. B., White, E. S., Lynch, J. P. & Martinez, F. J. Mechanisms of pulmonary fibrosis. *Annu. Rev. Med.* **55,** 395–417 (2004).

68. Huang, X. *et al.* Matrix stiffness-induced myofibroblast differentiation is mediated by intrinsic mechanotransduction. *Am. J. Respir. Cell Mol. Biol.* **47,** 340–8 (2012).

69. Zhou, Y. *et al.* Inhibition of mechanosensitive signaling in myofibroblasts ameliorates experimental pulmonary fibrosis. *J. Clin. Invest.* **123,** 1096–108 (2013).

70. Phan, S. H. The myofibroblast in pulmonary fibrosis. *Chest* **122,** 286S–289S (2002).

71. Kim, K. K. *et al.* Alveolar epithelial cell mesenchymal transition develops in vivo during pulmonary fibrosis and is regulated by the extracellular matrix. *Proc. Natl. Acad. Sci. U. S. A.* **103,** 13180–5 (2006).

72. Willis, B. C. *et al.* Induction of epithelial-mesenchymal transition in alveolar epithelial cells by transforming growth factor-beta1: potential role in idiopathic pulmonary fibrosis. *Am. J. Pathol.* **166,** 1321–32 (2005).

73. Larios, J. M., Budhiraja, R., Fanburg, B. L. & Thannickal, V. J. Oxidative protein

cross-linking reactions involving L-tyrosine in transforming growth factor-beta1-stimulated fibroblasts. *J. Biol. Chem.* **276,** 17437–41 (2001).

74. Hecker, L. *et al.* Reversal of persistent fibrosis in aging by targeting Nox4-Nrf2 redox imbalance. *Sci. Transl. Med.* **6,** 231ra47 (2014).

75. Moore, B. B. & Hogaboam, C. M. Murine models of pulmonary fibrosis. *AJP Lung Cell. Mol. Physiol.* **294,** L152–L160 (2007).

76. Umezawa, H., Ishizuka, M., Maeda, K. & Takeuchi, T. Studies on bleomycin. *Cancer* **20,** 891–5 (1967).

77. Umezawa, H. Chemistry and mechanism of action of bleomycin. *Fed. Proc.* **33,** 2296–302 (1974).

78. Muggia, F. M., Louie, A. C. & Sikic, B. I. Pulmonary toxicity of antitumor agents. *Cancer Treat. Rev.* **10,** 221–43 (1983).

79. Adamson, I. Y. Pulmonary toxicity of bleomycin. *Environ. Health Perspect.* **16,** 119–26 (1976).

80. Crystal, R. G. Lung collagen: definition, diversity and development. *Fed. Proc.* **33,** 2248–55 (1974).

81. Schrier, D. J., Kunkel, R. G. & Phan, S. H. The role of strain variation in murine bleomycin-induced pulmonary fibrosis. *Am. Rev. Respir. Dis.* **127,** 63–6 (1983).

82. Izbicki, G., Segel, M. J., Christensen, T. G., Conner, M. W. & Breuer, R. Time course of bleomycin-induced lung fibrosis. *Int. J. Exp. Pathol.* **83,** 111–9 (2002).

83. Janick-Buckner, D., Ranges, G. E. & Hacker, M. P. Alteration of bronchoalveolar lavage cell populations following bleomycin treatment in mice. *Toxicol. Appl. Pharmacol.* **100,** 465–73 (1989).

84. Phan, S. H. *et al.* A comparative study of pulmonary fibrosis induced by bleomycin and an O2 metabolite producing enzyme system. *Chest* **83,** 44S–45S (1983).

85. Lawson, W. E. *et al.* Increased and prolonged pulmonary fibrosis in surfactant protein C-deficient mice following intratracheal bleomycin. *Am. J. Pathol.* **167,** 1267–77 (2005).

86. Travis, E. L. *et al.* NRF2 deficiency reduces life span of mice administered thoracic irradiation. *Free Radic. Biol. Med.* **51,** 1175–83 (2011).

87. Franko, A. J., Sharplin, J., Ward, W. F. & Taylor, J. M. Evidence for two patterns of inheritance of sensitivity to induction of lung fibrosis in mice by radiation, one of which involves two genes. *Radiat. Res.* **146,** 68–74 (1996).

88. Sharplin, J. & Franko, A. J. A quantitative histological study of strain-dependent differences in the effects of irradiation on mouse lung during the early phase. *Radiat. Res.* **119,** 1–14 (1989).

89. Haston, C. K. & Travis, E. L. Murine susceptibility to radiation-induced pulmonary fibrosis is influenced by a genetic factor implicated in susceptibility to bleomycin-induced pulmonary fibrosis. *Cancer Res.* **57,** 5286–91 (1997).

90. Epperly, M. W., Guo, H., Gretton, J. E. & Greenberger, J. S. Bone marrow origin of myofibroblasts in irradiation pulmonary fibrosis. *Am. J. Respir. Cell Mol. Biol.* **29,** 213–24 (2003).

91. Jackson, S. H., Gallin, J. I. & Holland, S. M. The p47phox mouse knock-out model of chronic granulomatous disease. *J. Exp. Med.* **182,** 751–8 (1995).

92. Davies, S. S. *et al.* Localization of isoketal adducts in vivo using a single-chain antibody. *Free Radic. Biol. Med.* **36,** 1163–74 (2004).

93. Galligan, J. J. *et al.* Stable histone adduction by 4-oxo-2-nonenal: a potential link between oxidative stress and epigenetics. *J. Am. Chem. Soc.* **136,** 11864–6 (2014).

94. Kirabo, A. *et al.* DC isoketal-modified proteins activate T cells and promote hypertension. *J. Clin. Invest.* **124,** 4642–56 (2014).

95. Wu, J. *et al.* Immune activation caused by vascular oxidation promotes fibrosis and hypertension. *J. Clin. Invest.* **126,** 50–67 (2016).

96. Lane, K. L. *et al.* Oxidative injury is a common consequence of BMPR2 mutations. *Pulm. Circ.* **1,** 72–83 (2011).

97. Mont, S. *et al.* Accumulation of isolevuglandin-modified protein in normal and fibrotic lung. *Sci. Rep.* **6,** 24919 (2016).

98. Lambeth, J. D. NOX enzymes and the biology of reactive oxygen. *Nat. Rev. Immunol.* **4,** 181–9 (2004).

99. Jones, S. A. *et al.* Expression of phagocyte NADPH oxidase components in human endothelial cells. *Am. J. Physiol.* **271,** H1626–34 (1996).

100. Mi, H., Muruganujan, A. & Thomas, P. D. PANTHER in 2013: modeling the evolution of gene function, and other gene attributes, in the context of phylogenetic trees. *Nucleic Acids Res.* **41,** D377–86 (2013).

101. Carrier, E. J., Zagol-Ikapitte, I., Amarnath, V., Boutaud, O. & Oates, J. a. Levuglandin forms adducts with histone h4 in a cyclooxygenase-2-dependent manner, altering its interaction with DNA. *Biochemistry* **53,** 2436–41 (2014).

102. Collinson, E., Dainton, F. S. & Kroh, J. Effects of linear energy transfer on the radiolysis of water and heavy water. *Nature* **187,** 475–7 (1960).

103. Balli, D. *et al.* Foxm1 transcription factor is required for lung fibrosis and epithelial-to-mesenchymal transition. *EMBO J.* **32,** 231–44 (2013).

104. Phillips, T. L. An ultrastructural study of the development of radiation injury in the lung. *Radiology* **87,** 49–54 (1966).

105. Adamson, I. Y., Bowden, D. H. & Wyatt, J. P. A pathway to pulmonary fibrosis: an ultrastructural study of mouse and rat following radiation to the whole body and hemithorax. *Am. J. Pathol.* **58,** 481–98 (1970).

106. White, D. C. The histopathologic basis for functional decrements in late radiation injury in diverse organs. *Cancer* **37,** 1126–43 (1976).

107. Penney, D. P. & Rubin, P. Specific early fine structural changes in the lung irradiation. *Int. J. Radiat. Oncol. Biol. Phys.* **2,** 1123–32 (1977).

108. Moosavi, H. *et al.* Early radiation dose-response in lung: an ultrastructural study. *Int. J. Radiat. Oncol. Biol. Phys.* **2,** 921–31 (1977).

109. Fuks, Z. *et al.* Basic fibroblast growth factor protects endothelial cells against radiation-induced programmed cell death in vitro and in vivo. *Cancer Res.* **54,** 2582–90 (1994).

110. Davies, S. S. Modulation of protein function by isoketals and levuglandins. *Subcell. Biochem.* **49,** 49–70 (2008).

111. Kalash, R. *et al.* Amelioration of radiation-induced pulmonary fibrosis by a water-soluble bifunctional sulfoxide radiation mitigator (MMS350). *Radiat. Res.* **180,** 474–90 (2013).

112. Artaud-Macari, E. *et al.* Nuclear factor erythroid 2-related factor 2 nuclear translocation induces myofibroblastic dedifferentiation in idiopathic pulmonary

fibrosis. *Antioxid. Redox Signal.* **18,** 66–79 (2013).

113. Citrin, D. E. *et al.* Role of type II pneumocyte senescence in radiation-induced lung fibrosis. *J. Natl. Cancer Inst.* **105,** 1474–1484 (2013).

114. Zhao, W. & Robbins, M. E. C. Inflammation and chronic oxidative stress in radiation-induced late normal tissue injury: therapeutic implications. *Curr. Med. Chem.* **16,** 130–43 (2009).

115. Laleu, B. *et al.* First in class, potent, and orally bioavailable NADPH oxidase isoform 4 (Nox4) inhibitors for the treatment of idiopathic pulmonary fibrosis. *J. Med. Chem.* **53,** 7715–30 (2010).

116. Sener, G. *et al.* Ginkgo biloba extract protects against ionizing radiation-induced oxidative organ damage in rats. *Pharmacol. Res.* **53,** 241–52 (2006).

117. Davies, S. S. *et al.* Effects of reactive gamma-ketoaldehydes formed by the isoprostane pathway (isoketals) and cyclooxygenase pathway (levuglandins) on proteasome function. *FASEB J.* **16,** 715–7 (2002).

118. Roychowdhury, S. *et al.* Formation of gamma-ketoaldehyde-protein adducts during ethanol-induced liver injury in mice. *Free Radic. Biol. Med.* **47,** 1526–38 (2009).

119. Bernoud-Hubac, N. *et al.* Low concentrations of reactive gamma-ketoaldehydes prime thromboxane-dependent human platelet aggregation via p38-MAPK activation. *Biochim. Biophys. Acta* **1791,** 307–13 (2009).

120. Laskin, D. L., Malaviya, R. & Laskin, J. D. in *Comparative Biology of the Normal Lung* 793–794 (Elsevier, 2015). doi:10.1016/B978-0-12-404577-4.15011-8

121. Kim, H. G. *et al.* Endosulfan induces COX-2 expression via NADPH oxidase and the ROS, MAPK, and Akt pathways. *Arch. Toxicol.* **89,** 2039–50 (2015).

122. Sancho, P., Martín-Sanz, P. & Fabregat, I. Reciprocal regulation of NADPH oxidases and the cyclooxygenase-2 pathway. *Free Radic. Biol. Med.* **51,** 1789–98 (2011).

123. Iyer, R. S., Ghosh, S. & Salomon, R. G. Levuglandin E2 crosslinks proteins. *Prostaglandins* **37,** 471–80 (1989).

124. Murthi, K. K., Friedman, L. R., Oleinick, N. L. & Salomon, R. G. Formation of DNA-protein cross-links in mammalian cells by levuglandin E2. *Biochemistry* **32,**

4090–7 (1993).

125. Sidorova, T. N. *et al.* Reactive γ-ketoaldehydes promote protein misfolding and preamyloid oligomer formation in rapidly-activated atrial cells. *J. Mol. Cell. Cardiol.* **79,** 295–302 (2015).

126. Boutaud, O. *et al.* Prostaglandin H2 (PGH2) accelerates formation of amyloid beta1-42 oligomers. *J. Neurochem.* **82,** 1003–6 (2002).

127. Stavrovskaya, I. G. *et al.* Reactive gamma-ketoaldehydes formed via the isoprostane pathway disrupt mitochondrial respiration and calcium homeostasis. *Free Radic. Biol. Med.* **49,** 567–79 (2010).

128. Wynn, T. A. Cellular and molecular mechanisms of fibrosis. *J. Pathol.* **214,** 199–210 (2008).

129. Limper, A. H. Chemotherapy-induced lung disease. *Clin. Chest Med.* **25,** 53–64 (2004).

130. Zagol-Ikapitte, I. A. *et al.* Determination of the Pharmacokinetics and Oral Bioavailability of Salicylamine, a Potent γ-Ketoaldehyde Scavenger, by LC/MS/MS. *Pharmaceutics* **2,** 18–29 (2010).

131. Davies, S. S. *et al.* Pyridoxamine analogues scavenge lipid-derived gamma-ketoaldehydes and protect against H2O2-mediated cytotoxicity. *Biochemistry* **45,** 15756–67 (2006).

132. Davies, S. S. *et al.* Treatment with a γ-ketoaldehyde scavenger prevents working memory deficits in hApoE4 mice. *J. Alzheimers. Dis.* **27,** 49–59 (2011).

133. Shiber, A. & Ravid, T. Chaperoning proteins for destruction: diverse roles of Hsp70 chaperones and their co-chaperones in targeting misfolded proteins to the proteasome. *Biomolecules* **4,** 704–24 (2014).

134. Marshall, R. S. & Vierstra, R. D. Eat or be eaten: The autophagic plight of inactive 26S proteasomes. *Autophagy* **11,** 1927–8 (2015).

135. Erazo-Oliveras, A. *et al.* Protein delivery into live cells by incubation with an endosomolytic agent. *Nat. Methods* **11,** 861–7 (2014).

136. Chowdary, D. R., Dermody, J. J., Jha, K. K. & Ozer, H. L. Accumulation of p53 in a mutant cell line defective in the ubiquitin pathway. *Mol. Cell. Biol.* **14,** 1997–2003 (1994).

137. Yapici, N. B. *et al.* Highly stable and sensitive fluorescent probes (LysoProbes) for lysosomal labeling and tracking. *Sci. Rep.* **5,** 8576 (2015).

138. Lee, D. H. & Goldberg, A. L. Selective inhibitors of the proteasome-dependent and vacuolar pathways of protein degradation in Saccharomyces cerevisiae. *J. Biol. Chem.* **271,** 27280–4 (1996).

139. Wutz, A. Epigenetic regulation of stem cells : the role of chromatin in cell differentiation. *Adv. Exp. Med. Biol.* **786,** 307–28 (2013).

140. Charvet, C. D. & Pikuleva, I. A. Mass spectrometry detection of isolevuglandin adduction to specific protein residues. *Methods Mol. Biol.* **1208,** 285–98 (2015).

141. Hu, N. *et al.* Abnormal histone modification patterns in lupus CD4+ T cells. *J. Rheumatol.* **35,** 804–10 (2008).

142. Zhang, P., Su, Y., Zhao, M., Huang, W. & Lu, Q. Abnormal histone modifications in PBMCs from patients with psoriasis vulgaris. *Eur. J. Dermatol.* **21,** 552–7

143. Xiaomeng, X., Ming, Z., Jiezhi, M. & Xiaoling, F. Aberrant histone acetylation and methylation levels in woman with endometriosis. *Arch. Gynecol. Obstet.* **287,** 487–94 (2013).

144. Wang, Y. *et al.* Aberrant histone modification in peripheral blood B cells from patients with systemic sclerosis. *Clin. Immunol.* **149,** 46–54 (2013).

145. Zhao, H., Xue, F., Xu, J. & Fang, Z. Aberrant histone methylation in the patients with immune thrombocytopenia. *Platelets* **25,** 207–10 (2014).